UNIVERSIDADE DA CORUÑA

Facultade de Ciencias

Chemistry Degree/ Grado en Química/ Grao en Química

Memoria do Traballo de Fin de Grao

Desing of new antimicrobials based on iron chelating agents

Diseño de nuevos antibióticos basados en agentes quelantes de hierro

Diseño de novos antibióticos baseados en axentes quelantes de ferro

Natalia Montero Sánchez-Campins

Curso: 2023 - 2024

Convocatoria: Febreiro

Directores: *Jaime Rodríguez González*

Carlos Jiménez González

Agradecimientos

En primer lugar, a mis tutores Carlos Jiménez González y Jaime Rodríguez González por su orientación, sus conocimientos e inspiración. Al grupo de investigación PRONAMAR por crear un ambiente tan cómodo que facilitó mi trabajo y mi aprendizaje. Un agradecimiento especial va dirigido a Ana Rodríguez Pedrouzo, quien ha estado dispuesta a enseñarme y ayudarme en todo momento.

También quiero agradecer a mis amigas de toda la vida por su constante respaldo y compañía. Siempre han sido un pilar fundamental.

A las personas que han sido parte de mi día a día en esta etapa universitaria, contribuyendo de diversas maneras a mi desarrollo personal y académico. Recordaré con gratitud los momentos compartidos.

Y, por supuesto, mi más profundo agradecimiento a mi familia por su apoyo y cariño incondicional. Por incentivarme y confiar en mí continuamente.

Gracias a todos por ser parte de este estimable proceso.

ABBREVIATIONS AND ACRONYMS

δ Chemical shift

COSY Correlation spectroscopyc

cUTI Complicated urinary tract infections

d Doublet

Da Dalton

dd Double doublet

DMF N,N-Dimethylformamide

DNA Deoxyribonucleic acid

ESI Electrospray ionisation

FAO Food and Agriculture Organization of the United Nations

FDA U.S. Food and Drug Administration

h Hours

hept Heptaplet

HR High Resolution

HSQC Heteronuclear single quantum coherence spectroscopy

Hz Hertz

iPr Isopropyl

J Coupling constant

Kps Solubility constant

M Molar

m Multiplet

M Methyl

MHz Megahertz

MS Mass spectrometry

m/z Mass-to-charge ratio

O Oxazole

OIE World Organisation for Animal Health

OZ Oxazoline

PBP Periplasmic binding protein

PG Peptidoglycan

pka Acid dissociation constant

PNUMA United Nations Environment Program

ppm Parts per million

q Quadruplet

AMR Antimicrobial resistance

NMR Nuclear Magnetic Resonance

s Singlet

STD Standard deviation

subsp. Subspecies

t Triplet

T Thiazole

TBTU 2-(1H-benzotriazol-1-yl)-1,1,3,3-tetramethyluronium tretrafluoroborate

TD Thiazolidine

TLC Thin layer chromatography

TZ Thiazoline

UV Ultraviolet

Ycb Yersiniabactin

WHO World Health Organization

TABLE OF CONTENTS

ABSTRACT

The widespread use of antibiotics has contributed to the spread of antimicrobial resistance (AMR), necessitating the development of new, more effective drugs. Narrow-spectrum antibiotics that target specific pathogens are critical to delay the development of bacterial resistance. AMR is a significant global threat to public health, animal production, and economic and agricultural development. In this context, the study of siderophores such as piscibactin (Pcb, **1**) and yersiniabactin (Ycb, **2**) is relevant. Piscibactin (Pcb) is a phenolate-type siderophore responsible for Fe^{3+} uptake by the bacteria *Photobacterium damselae subsp. piscicida* and *Vibrio anguillarum*. Its low stability hinders its biotechnological applications, making the preparation of stable analogues of Ga^{+3}-coordinated Pcb indispensable for their development. The structure of Pcb is very similar to that of yersiniabactin (Ycb), a siderophore involved in iron uptake by certain pathogenic *Yersinia* species such *as Y. pestis*, the causative agent of bubonic plague and *Y. enterocolitica*, known to cause severe enteric disorders in humans.

In this work we propose to synthesize an advanced intermediate that can be used by the research group in the synthesis of a simplified and stable analogue of Pcb that will allow in the future to develop new biotechnological applications. It was decided to prepare the analogue T_OZ_T (thiazole-oxazoline-thiazole). All the synthesized compounds were characterized both by NMR and mass spectrometry.

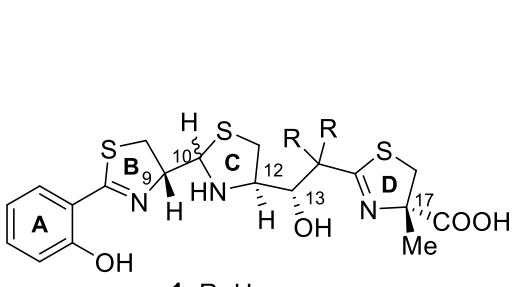

1, R=H
2, R=Me

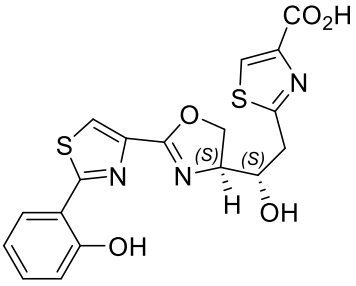

Analogue Pcb T_OZ_T

Key words: siderophore, piscibactin, yersiniabactin, T_OZ_T analogue.

RESUMEN

El uso generalizado de antibióticos ha contribuido a la propagación de resistencia a los antimicrobianos (RAM), siendo necesario el desarrollo de nuevos fármacos más efectivos. Los antibióticos de espectro reducido que se dirigen a patógenos específicos son fundamentales para retrasar el desarrollo de resistencia bacteriana. La RAM es una amenaza global significativa para la salud pública, la producción animal y el desarrollo económico y agrícola. En este contexto, el estudio de sideróforos como la piscibactina (Pcb, **1**) y la yersiniabactina (Ycb, **2**) resulta relevante. La piscibactina (Pcb) es un sideróforo de tipo fenolato responsable de la captación de Fe^{3+} de las bacterias *Photobacterium damselae subsp. piscicida* y *Vibrio anguillarum*. Su baja estabilidad dificulta sus aplicaciones biotecnológicas, por lo que se hace indispensable la preparación de análogos estables de Pcb coordinado con Ga^{3+} para poder desarrollarlas. La estructura de Pcb es muy similar a la de yersiniabactina (Ycb), un sideróforo involucrado en la captación de hierro por ciertas especies patógenas de *Yersinia* como *Y. pestis*, el agente causal de la peste bubónica y *Y. enterocolitica*, conocida por causar trastornos entéricos graves en humanos.

En este trabajo se propone sintetizar un intermedio avanzado que pueda ser utilizado por el grupo de investigación en la síntesis de un análogo simplificado y estable de Pcb que permita en un futuro desarrollar nuevas aplicaciones biotecnológicas. Se decidió preparar el análogo T_OZ_T (tiazol-oxazolina-tiazol). Todos los compuestos sintetizados se caracterizaron tanto por RMN como por espectrometría de masas.

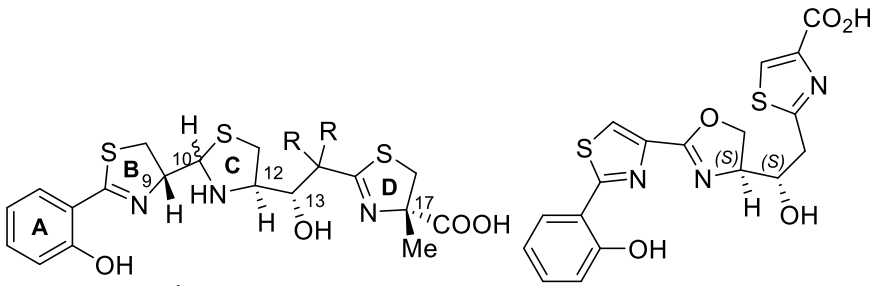

1, R=H
2, R=Me

Analogue Pcb T_OZ_T

Palabras clave: sideróforo, piscibactina, yersiniabactina, análogo T_OZ_T.

RESUMO

O uso xeneralizado de antibióticos contribuíu á propagación da resistencia aos antimicrobianos (RAM), polo que é necesario desenvolver novos fármacos máis eficaces. Os antibióticos de espectro estreito que teñen como obxectivo patóxenos específicos son esenciais para atrasar o desenvolvemento da resistencia bacteriana. A RAM é unha ameaza global importante para a saúde pública, a produción animal e o desenvolvemento económico e agrícola. Neste contexto, é relevante o estudo de sideróforos como a piscibactina (Pcb, **1**) e a yersiniabactina (Ycb, **2**). A piscibactina (Pcb) é un sideróforo de tipo fenolato responsable da captación de Fe^{3+} pola bacteria *Photobacterium damselae subsp. piscicida* e *Vibrio anguillarum*. A súa baixa estabilidade dificulta as súas aplicacións biotecnolóxicas, polo que a preparación de análogos estables de Pcb coordinados con Ga^{3+} é fundamental para poder desenvolvelos. A estrutura da Pcb é moi similar á da yersiniabactina (Ycb), un sideróforo implicado na captación de ferro por certas especies patóxenas de *Yersinia* como *Y. pestis*, o axente causante da peste bubónica, e *Y. enterocolitica*, que se sabe que causa trastornos entéricos graves en humanos.

Neste traballo proponse sintetizar un intermedio avanzado que poida ser utilizado polo grupo de investigación na síntese dun análogo simplificado e estable de Pcb que permita nun futuro desenvolver novas aplicacións biotecnolóxicas. Decidiuse preparar o análogo T_OZ_T (tiazol-oxazolina-tiazol). Todos os compostos sintetizados caracterizáronse tanto por RMN como por espectrometría de masas.

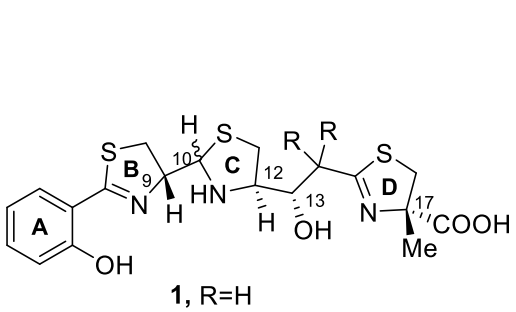

1, R=H
2, R=Me

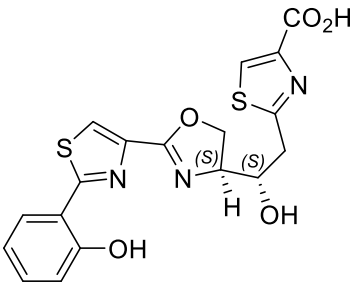

Analogue Pcb T_OZ_T

Palabras chave: sideróforo, piscibactina, yersiniabactina, análogo T_OZ_T.

1 INTRODUCTION

1.1 The Bubonic Plague and *Yersinia pestis*

The Black Death, the plague that killed about 50 million people in Europe in the 14th to 18th centuries, is still a problem today. The Bubonic plague infectious disease is caused by the bacterium *Yersinia pestis*; a Gram-negative short bacillus usually found in wild rodents, fleas that parasitize them and carnivores that ate the infected animals. Although it has been controlled for more than six centuries by different environmental and medical factors, plague continues to reemerge in sporadic cases or limited outbreaks. Between 2010 and 2015, 3248 cases were reported worldwide, 584 of them fatal. Currently, the three most endemic countries are Madagascar, the Democratic Republic of Congo and Peru.[1,2,3]

There are two main clinical forms caused by the agent: bubonic and pneumonic. Bubonic, the most common form, is transmitted through the bite of fleas or infected animals, or even, with the contact of their fluids or tissues. On the other hand, (primary) pneumonic transmission occurs by inhalation of respiratory particles from patients with lung infection which are extremely virulent. Bubonic plague can progress and spread to the lungs producing haematogenous (secondary) pneumonic plague. The incubation period for primary pneumonic plague can be as short as 24 h unlike the bubonic that can reach 7 days. Pneumonic plague can also be transmitted through exposure in a laboratory or intentional spread of aerosols as an act of bioterrorism.[1,3]

The general symptoms are fever, headache, and weakness, with other nonspecific systemic symptoms. The difference related to each type and name are the appearance of swollen, painful lymph nodes (called buboes), and a rapidly developing pneumonia.[1,3] "The Black plague" name is referred to the fact that it causes gangrene in certain parts of the body, such as the fingers and toes, which end up completely blackened.[4]

As the symptoms are difficult to identify in time because of their similarity to flu, diagnosis is made by taking samples of pus from a bubo, blood, or sputum from the patient, and submitting them for laboratory testing. As prior vaccination does not prevent plague, OMS does not recommend vaccination, except for high-risk groups such as health professionals.[1,3]

This plague can be a very serious disease for humans because, in the absence of prompt treatment, bubonic plague has a case fatality rate of 30% to 60%, and pneumonic plague is invariably fatal, particularly contagious, and capable of triggering severe epidemics. Fortunately, antibiotic treatment is effective against Enterobacteriaceae (Gram-negative bacilli), and bubonic plague can be treated and cured with these antibiotics under hospitalization. In some cases, you may be put into an isolation unit.[1,3] Some antibiotics that treat bubonic plague include Ciprofloxacin, Levofloxacin and Moxifloxacin, and Gentamicin.[3,5]

1.1.1 The Black Death Begins

In January 1348, attacking ships coming from Mongolia infected Genova by a second plague while already battling the previous one. This was determinant for the rest of Europe, Middle East, and North Africa, on a large scale until 1353.[6]

In 1266, the auge of Medieval European commercial expansion, Mongols gave up land in Caffa (currently Feodosia, Crimea Peninsula) to Genoeses. However, starting the next century, the Empire was fragmented by the conversion to Islam leading to clashes with Christians and wanting to expel the Europeans. In 1346, the warriors contracted the bacteria from Central Asia and the army catapults the infected bodies of their dead over city walls also condemning his opponents.[7] Soon all the air was infected, and the water poisoned, such a pestilence developed that barely one in a thousand managed to escape. Constantinople (currently Istanbul), Sicilia and France, were the principal affected this time.[6]

When the first hot weather arrived, the situation worsened. The people were either in prayer or madness, thinking it was the Apocalypse.[8] Superstitions blamed on the Jews; they were burned in their thousands. In Germany and France, Jewish communities were annihilated. Poland, Lithuania and Marseille were a haven to persecuted Jews, initiating a mass migration.[6]

In 1351, the plague's spread significantly begins to peter out, possibly thanks to quarantine efforts, after causing the deaths of anywhere between 25 to 50 million people and leading to the massacres of 210 Jewish communities. All total, Europe has lost about 50 percent of its population.[6,8]

In 1353, the people of Europe face a changed society. The average standard of living rose and new ideas and art concepts took hold, leading to the Renaissance and a more youthful, enlightened period.[6]

The Bubonic Plague never completely exits, resurfacing several times through 500 years, which together are called the Second Plague Pandemic.[6,9]

Recent studies from 2020, confirms that the firsts case of Bubonic plague was in 1338 in Kyrgyzstan. [9,10]

1.1.2 The final battle against the plague

It was more than five hundred years before Pasteur, in 1879, proposed the search for the microbe that caused the Plague. At that time, it was less fatal than in the Middle Ages, but still wreaked havoc. Thus, it was that Yersin, a collaborator of Roux (director of the Pasteur Institute) and a disciple of Pasteur, decided to leave in 1894 to Hong-Kong. There he met Shibamiro Kitasato, a disciple of Koch. An old polemic between Pasteur and Koch, which had affected the scientific field on numerous occasions, could have been resumed. Fortunately, the common enemy imposed a truce between them. Yersin modified the Gram stain that Kitasato was using to methylene blue to visualise the bacillus, evidencing its aerobic nature. [11]

The next step was to find out where the disease came from. It was known that mainly the transmission in hospitals was through coughing (pneumonic plague) while in the neighbourhoods this did not occur (bubonic plague). In 1897, the bacteriologist Hankin noted that in Mumbai (formerly known as Bombay), India's most populous port city, only the prisoners and jailers in Byculla prison had not been infected because of their isolation. He discovered that the human plague came from a murine plague in rats. At first, the rats in contact with the prison were not infected because they lived in separate sewers from the sick ones. When they contracted the bacteria, Hankin verified his hypothesis by taking into account the incubation time.[11]

This means of transmission could explain the spread of the epidemic in countries separated by the sea. *Mus Decumanus* rats are good swimmers and, being able to withstand humidity and darkness, are regular guests in the holds of ships, explaining why it could affect the inhabitants of the towns where the ship stops and not the crewmembers.

Strangely, there were cases where people were infected after the death of the sick person at the wake and not when they were caring for them. This turned out to be due to fleas leaving the dead body and seeking to live with another.

Around 1898, Yersin, Calmette, and Haffkine succeeded in preparing the first vaccines against the plague putting an end as pandemic.[11]

1.1.3 Plague Worldwide

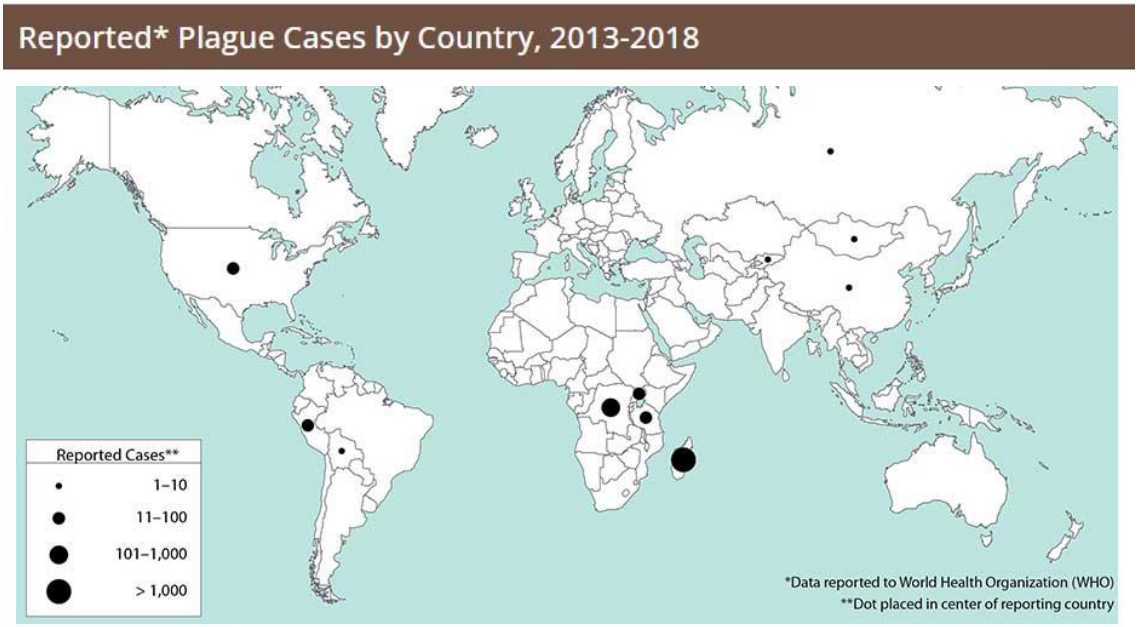

Figure 1. Reported Plague cases by Country, 2013 and 2018. [12]

As an animal disease, plague is present on all continents except Oceania. Plague epidemics have occurred in Africa, Asia, and America between 2013 and 2018 *(Figure 1)*, but most human cases since the 1990s have occurred in Africa. Almost all the cases reported in the last decades have occurred among people living in small towns and villages or agricultural areas rather than in larger towns and cities.[12]

In Madagascar in 2017, more than 300 cases were detected.[13] Here cases of bubonic plague are reported almost every year during the epidemic season (between September and April).[1] During the Covid-19 crisis in 2020, a city in one of China's autonomous regions, Mongolia Interior, was declared on precautionary alert after a confirmed case of bubonic plague. This situation has previously occurred by marmot meat intake in 2019, but this time had a higher importance to eradicate it due to the economic, sanity and humanitarian circumstances wreaked by Covid-19.[4] It is worth to mention that the average of seven human plague cases in the United States reported each year (range: 1–17 cases per year) where most human cases occur in two regions: Northern New Mexico, northern Arizona, and southern Colorado; and California, southern Oregon, and far western Nevada.[5,12] Over 80% plague cases have been the bubonic form and many of the cases have been developed by domestic animals that ate rats bearing bacteria, especially cats.[3,12] The last urban plague epidemic associated with rats in the United States occurred

in Los Angeles from 1924 through 1925. Studies confirm that affects indistinct to age and sex, although men around 12 and 45 years are historically more probably to be infected because of increased outdoor activities that put them at higher risk.[12]

1.2 Antibiotic Resistance

Antimicrobial Resistance (AMR) is the ability of microorganisms to resist antimicrobial treatments, especially antibiotics, which they were previously susceptible on a count of a consequence of natural selection and genetic mutation.[14,15] Superbugs are the biggest threat to human health in the coming years.[16] Even though this problem has existed for decades, the global consumption of antibiotics in human medicine increased by almost 40% between 2000 and 2010. By 2050, antibiotic resistance will be responsible around 10 million deaths annually if current infection and resistance trends are not reversed. The largest numbers will be in Africa and Asia *(Figure 2).* If trends continue, we would revert to a world where simple infections are no longer treatable.[14,15,16]

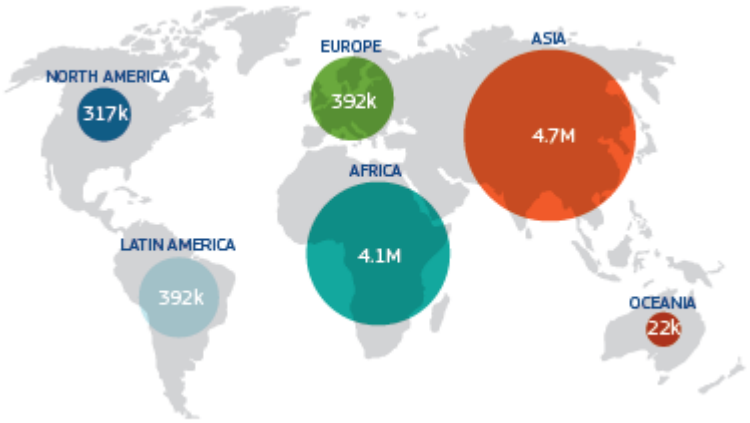

Figure 2. Number of deaths per year attributable to AMR by 2050 if current resistance rates increased by 40%. [14]

AMR not only affects human health, animals, food, and the environment, but it also has an economic cost. The extra healthcare costs and productivity losses due to multidrug-resistant bacteria causes EUR 1.5 billion each year in the EU. An example for Trade and Agriculture losses; in 2015 chicken sales in Norway dropped by 20% (for some distributors) following the news that a resistant strain of *Escherichia coli (E. coli)* was found in chicken meat.[14]

Another important fact is that the bulk of antimicrobials are not consumed by humans, it is by animals affecting us laterally. Only 25% of countries have implemented a national policy

to tackle AMR and less than 40% of countries have put in place infection prevention and control programmes. Globally, it is estimated that only half of antibiotics are used correctly.[14]

Over 2011 Commission action plan, notable for its One Health approach (the term that recognise that humans, animals, and environment are interconnected), a new and comprehensive EU action plan on AMR was adopted on 29 June 2017. This will support the EU and its Member States a best practice Region; boosting it to research, development, and innovation. Its overarching goal is to preserve the possibility of effective treatment of infections in humans and animals. The new plan contains more than 75 concrete actions to combating AMR. It provides a framework for continued, more extensive action to reduce the emergence and to increase the development and availability of new effective antimicrobials inside and outside the EU.[15] As global cooperation is a key element of the AMR action plan, many countries outside of the EU, as well as international organisations, are tackling this issue: World Health Organization (WHO), World Organisation for Animal Health (OIE), Food and Agriculture Organization of the United Nations (FAO), United Nations Environment Program (PNUMA), and Codex Alimentarius.[14,17]

While antimicrobials (antibiotics, antivirals, antifungals, and antiprotozoals) are active substances of synthetic or natural origin which kill or inhibit the growth of microorganisms, superbugs are these microorganisms genetically evolved to be resistant to antibiotics and, in the presence of them, will reproduce and generate new infections more difficult to fight.[15,18]

Pharmaceutical companies must recuperate research and development investments selling their medicinal products. But this suppose a problem because if the new antimicrobial treatment is sold and used in large quantities, resistance can be expected to develop quickly. For this reason, a responsible use must be incorporated.[15]

Some measures are based on improving hygiene in the population, reducing the use of unnecessary antibiotics in human and veterinary medicine, and comply with medical prescription. Rapid and reliable diagnostics are crucial for differentiating between bacterial and viral infections and identifying AMR and help to reduce the unnecessary use of antimicrobials in humans and animals. [15]

At the same time of this wrong habits, historical data show a low success rate about the discovery, development, manufacture, and marketing of new antimicrobials in the past 20 years: only 1 out of 16 antibiotics from early-stage research reaches clinical application for patients.[15] Consequently, the other measure is in the field of research becoming one of the major challenges facing medicine. It would involve the development of new molecules, drugs, active centres and vaccines to deal with it.[16]

The broad-spectrum antibiotics act on highly conserved therapeutic targets. It´s present in many bacterial pathogens leading to resistance through various mechanisms such as the modification of the drug target, enzyme catalyzed antibiotic modifications, molecular bypass, and active efflux (or decreased entry) from the cell.[19] However, the use of narrow-spectrum antibiotics that target specific pathogens delays the emergence of bacterial resistance. This is another reason why it is necessary to design new antibiotics methodologies.

1.3 The role of Iron in bacterial development

Iron is required for the growth of nearly all bacterial species, being a crucial element for aerobic life. In most cells, Fe has multiple essential roles in biological processes such as nucleic acid synthesis, DNA repair, gene regulation, and oxygen transport. This element also acts as a cofactor for various metabolic enzymes due to its redox chemistry.[20-22]

Despite its high abundance in the earth's crust, iron is mostly found at physiological pH in its oxidized form Fe^{3+}. Unfortunately its bioavailability is limited by the low solubility of Fe(III) at near neutral pH ($K_{ps} = 10^{-39}$), precipitating as $Fe(OH)_3$, and its bioavailability decreases.[22,23]

To overcome this problem, microorganisms under iron limited conditions, have developed different strategies including one that synthesize and excrete low molecular weight molecules (500-1500 Da) into the extracellular medium in order to chelate iron (III), called siderophores. [23,24]

1.3.1 Siderophores

Siderophores, which are specific Fe(III)-binding agents, are produced by many but not all microorganisms in response to a deficiency of iron, forming soluble complexes. It has been shown that the production of siderophores is a key virulence factor for a potentially pathogenic bacterium to develop the infectious process.[25]

Siderophores have functional groups with oxygen and electron-donating nitrogen atoms, and a structure that allows them to act as hexadentate ligands and to form octahedral complexes with Fe^{3+}. Bacteria can biosynthesis more than one type of siderophore and use one or the other depending on the conditions of their environment, temperature, pH or the presence of other microorganisms. The pKa values determine their affinity for Fe^{3+}.[22,24]

Bacterial siderophores can be divided into three major families based on the chemical nature of the bidentate ligands involved in iron binding: catecholate, hydroxamate and carboxylates.[25]

Some siderophores, such as yersiniabactin and pyochelin, are considered to be ‘‘mixed type’’ siderophores, with chemical groups of two or more siderophore families *(Figure 3).*[25]

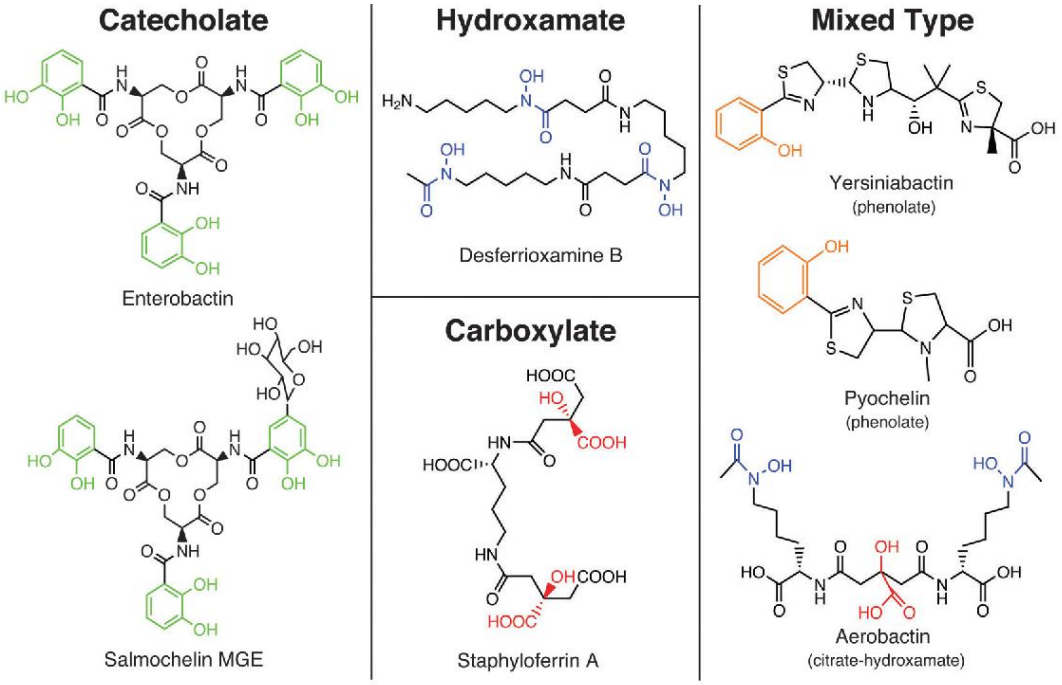

Figure 3. Siderophore´s structural families.[25]

The process starts with the secretion of these siderophores forming Fe(III)-siderophore complexes. By ferric-chelate-specific transporters, the complexes are taken into the cell, where ferric reductase enzymes catalyze the reduction of Fe(III) into Fe(II), triggering the release of Fe(II) ion, which is the soluble and the accessible form for the microorganism. Regulated by the iron levels of the environment, the siderophore can either be degraded or released in the free form outside the cell *(Figure 4).* [26]

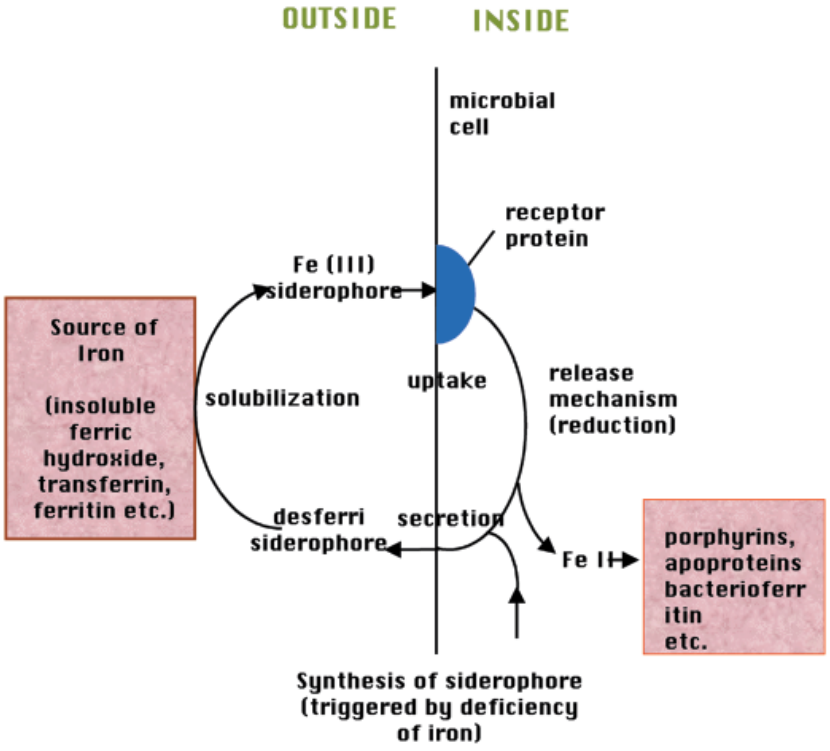

Figure 4. The siderophores system works.[27]

These molecules present another important biological functions as transport of non-metals or metals different than iron, detoxification of bacteria environment, interfering with quorum sensing, regulation, anticancer agents…[22,28] However, the antibiotic property is playing an important role in the development of numerous biotechnology applications in medicine. One of the most notable, it´s the use of the Troyan horse strategy for the design of new antimicrobials.[23,28]

1.3.2 Trojan horse strategy

One way to increase the efficiency of antibiotics is targeting because resolve the consequences of broad-spectrum antibiotic use on microbiome stability and pathogen resistance.[23,29] Specifically, the gram-negative bacteria *Acinetobacter baumannii*, *Pseudomonas aeruginosa* and *Enterobacteriaceae*, worrisome infections considered by the WHO, in which their pathogenicity increase via the compromised immune system of patients.[26]

Penicillin-binding proteins (PBPs) are membrane-associated proteins involved in the biosynthesis of peptidoglycan (PG), the main component of bacterial cell walls. Its name is due to its discovery of the capability to bind the β-lactam antibiotic penicillin. The low affinity of altered PBPs with β-lactam antibiotics or β-lactamases to inactivate the antibiotic are the major causes of resistance. Therefore, cell wall synthesis proceeds despite the presence of otherwise inhibitory concentrations of β-lactam antibiotics, thus evading cell death and lysis.[30,31]

The covalently bond between antibiotics and iron scavengers (siderophores), facilitate the internalization into the cell by using bacterial iron uptake pathways as gateways to introduce the drug in the bacteria. In addition to its entry into bacteria through porin channels like some drugs, the formation of the siderophore iron complex allows to easily enter through active iron transport system. Furthermore, it has proposed that in this way it is possible to avoid the resistance mechanisms, such as efflux pumps, porins, and ß-lactamases, and consequently reaching high concentrations in the periplasmic space. Once inside the bacterial cell, the drug can interact with peptidoglycan binding to BPB-3 and PBP-2 *(Figure 5).*[26,32]

This approach has proven to be particularly useful for precise delivery of β-lactam antibiotics, which represent about 70% of antibiotics prescribed today. The first antibiotic approved by the FDA for humans based on this principle was cefiderocol, a cephalosporin siderophore substituted which is used for treating complicated urinary tract infections (cUTI) when no other methods are available.[26,33]

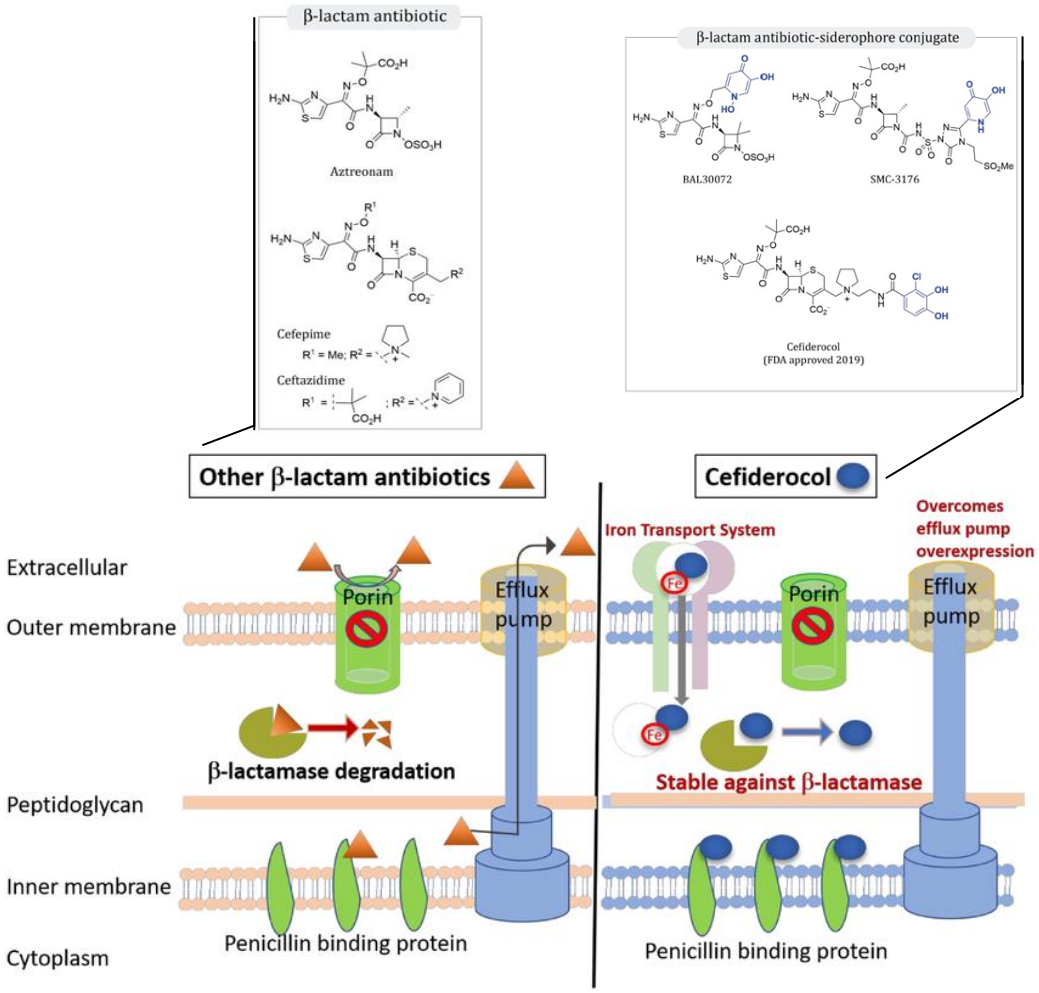

Figure 5. Mechanism of action without (left) and with (right) Trojan horse strategy.[26,33]

1.3.3 Siderophore of *Yersinia pestis* and *Yersinia enterocolitica*

The human pathogenic *Yersinia* (*Y. pestis, Y. pseudotuberculosis, and Y.enterocolitica*) can be grouped by its pathogenic. The two fist ones and *Y.enterocolitica* biogroup 1B make up the highly virulent group (strains able to kill mice at low infection doses). This indicates the ability of bacteria to express an efficient siderophore yersiniabactin (Ybt) that plays a significant role in iron acquisition and murine pathogenicity. In contrast, two other pathogroups (low and apathogenic) do not produce Ybt.[34]

Yersinia enterocolitica, a bacteria transmitted mainly by pigs, produces yersiniosis when passed to humans, the third most recorded zoonosis in the European Union in 2013. Most frequently affects young children and symptoms include fever, abdominal pain, and diarrhea.[35]

Yersinia pestis encodes a multitude of Fe transport systems that can be divided in four categories: heme uptake systems, ferric ABC transporters, ferrous transporters, and siderophore systems. Indeed, only yersiniabactin (Ybt siderophore) and Yfe and Feo (ferrous transporters) have been shown to be important in at least one form of plague. [20]

Figure. Yersinia enterocolitica (left) and Yersinia pestis (right).[36,37]

The Ybt system is encoded on a pathogenicity island and is functional in several different Gram-negative pathogens. Early research on the Ybt system focused on *Y. enterocolitica* and *Y. Pestis*.[20]

Yersiniabactin contains a phenolic group and three five-membered heterocycles that serve as iron ligands. Like other siderophores, Ybt has no affinity for ferrous iron. Its affinity for ferric iron (closely to 4×10^{36}) is higher than a number of other siderophores, indicating that Ybt should be able to remove iron from a variety of host ironbinding proteins.[38] A role for the Ybt siderophore in Zn acquisition has been revealed. Ybt-dependent Zn acquisition uses a transport system completely independent of the Fe-Ybt uptake system.[20] The absolute configuration of natural Ybt has been determined as 9*R*, 10*RS*, 12*R*, 13*S* and 19*S* *(Figure 6).* Diastereomers (isomers I and II) in regard to its C-10 configuration are unified into a single stereoisomer through gallium and aluminium.[39]

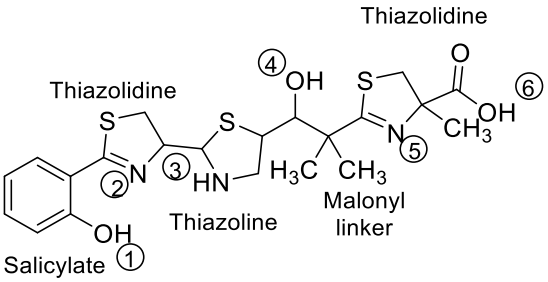

Figure 6. Structure of the Ybt siderophore. The six coordinate binding sites for Fe^{3+} are shown.

1.3.4 Piscibactin siderophore

The piscibactin siderophore is a key virulence factor involved in the bacteria *Photobacterium damselae subsp. piscicida* and *Vibrio anguillarum*, responsible for the fish diseases photobacterioisis (pasteurellosis) and vibriosis, respectively. Pcb is closely structurally related to the yersiniabactin (Ybc) and pyochelin siderophores.[28,29]

The structure of Pcb comprises two thiazoline rings (B and D), one thiazolidine ring (C) and bears five stereogenic centers. The difference with Ycb is that it lacks two methyl groups at the C14 position. The presence of the labile TD (C-ring) and the acid-sensitive fragment of TZ (D-ring) could explain the low stability of Pcb. With this aim the design of a simplified Pcb analogue that preserves the chelation of Fe^{3+} and mantains the siderophore activity, was proposed. In this way, the Pcb analague T_OZ_T (thiazole-oxazoline-thiazole) complex instead of TZ_TD_TZ (thiazoline-thiazolidine-thiazoline) complex was designed *(Figure 7).*[22]

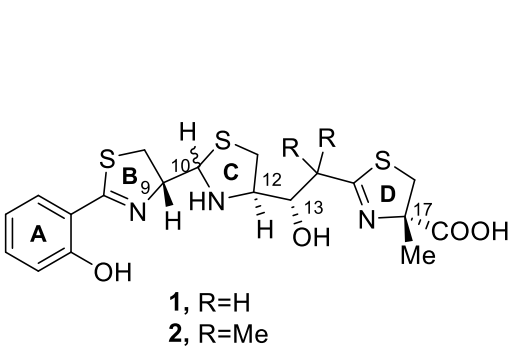

*Figure 7. Structure of piscibactin **(1)**, yersiniabactin **(2)** and the Ga^{3+} complex of Pcb analague.*[22]

2 OBJECTIVES

The final goal of this Thesis Degree is the search for a Ybt analogue to be used as a vector in the preparation of a conjugate following the Trojan horse strategy. To make this possible, the following specific objectives were set:

- The preparation of an advanced intermediate in the synthesis of a Pcb analogue where the structure of Pcb (TZ_TD_TZ) is substituted for a more simple structure (T_OZ_T) but keeping the same 13*S* configuration. This endeavor aims to develop new strategies for the detection or elimination of pathogenic Pcb-producing bacteria.

- Structural characterization of all the preparation of that advanced intermediate for the synthesis of the simplified analogue of Pcb.

3 RESULTS AND DISCUSSION

This section shows the synthetic route carried out for the preparation of the advanced intermediate for the synthesis of the simplified analogue of Pcb and the results obtained.

The main goal was the synthesis of a simplified analogue of Pcb that could chelate Fe3+, and keep the siderophores activity, and be more stable than Pcb. As demonstrated by computational methods in previous studies, performed by our research group PRONAMAR at CICA, this more stable analogue will be T_OZ_T (thiazole-oxazoline-thiazole) instead of TZ_TD_TZ (thiazoline-thiazolidine-thiazoline), the corresponding structure with Pcb. The thiazolidine or thiazoline rings, which are more unstable due to their easy hydrolysis or oxidation, will be replaced by thiazole or oxazole rings which are more stable, due to their aromatic character. Furthermore, they have the ability to form octahedral complexes with Fe^{3+} or Ga^{3+} as it was deduced by computational calculations. It is important to mention the preference of preparing Ga^{3+} complexes instead of Fe^{3+} because they can be studied by means of NMR techniques.

3.1 RETROSYNTHETIC ANALYSIS OF THE PCB ANALOGUE T_OZ_T (THIAZOLE-OXAZOLINE-THIAZOLE)

The B and D rings of thiazoline (TZ) would be replaced by thiazole (T) rings while the C ring of thiazolidine (TD) would change for an oxazoline (OZ) was proposed *(Figure 7).* The 13*S* configuration would be maintain and the preparation of the thiazole ring before the formation of oxazoline (OZ) was proposed *(Scheme 1).*[22]

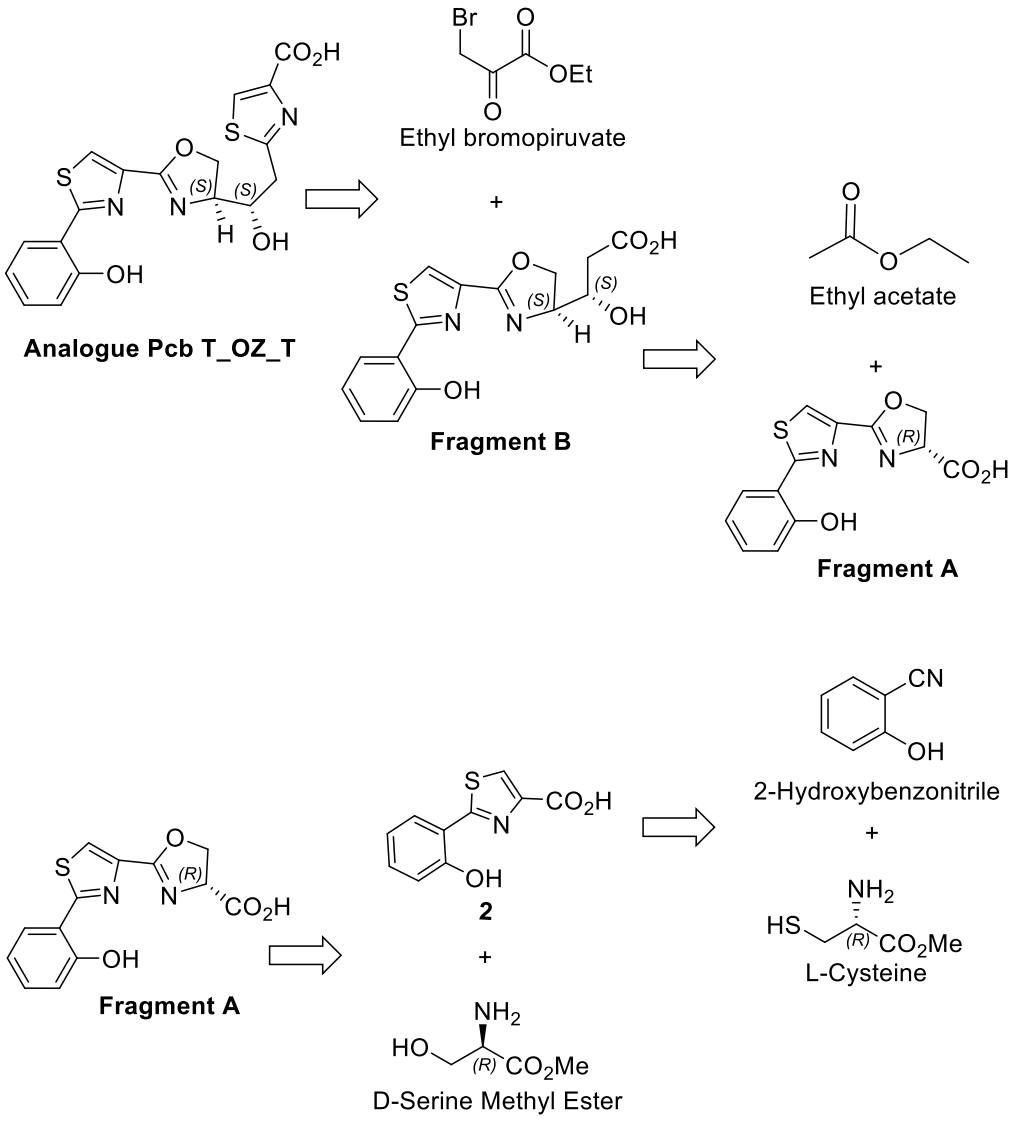

Scheme 1. Retrosynthetic analysis of the Pcb analogue T_OZ_T

The Hantzsch thiazole formation methodology from fragment B and ethyl bromopyruvate would be used to form the terminal T in ring D. Fragment B would be formed from the coupling between fragment A and ethyl acetate. The OZ ring C of fragment A would be obtained from the coupling of compound **2** with the methyl ester of D-serine. The T of compound **2** is formed from the oxidation of the TZ resulting from the coupling between 2-hydroxybenzonitrile and L-cysteine.[22]

3.2 PREPARATION OF THE PCB ANALOGUE T_OZ_T

Thiazolinic carboxylic acid **1** was obtained by the reaction at 65 °C of 2-hydroxybenzonitrile and L-cysteine, which acts as a chiral source of the 9*R* position, in a 1:1 mixture of MeOH in a phosphate buffer adjusted to pH 6.4 *(Scheme 2).*[22] Although 60 °C which was used in previous studies, increasing the temperature to 65 °C improved reaction yield. The most characteristic signal of **1** in its ^{1}H-NMR spectrum is H9, a triplet (*J* = 9.0 Hz) at 5.41 ppm, corresponding to the carbon proton at the α-position to the carboxylic group, which indicated ring formation.

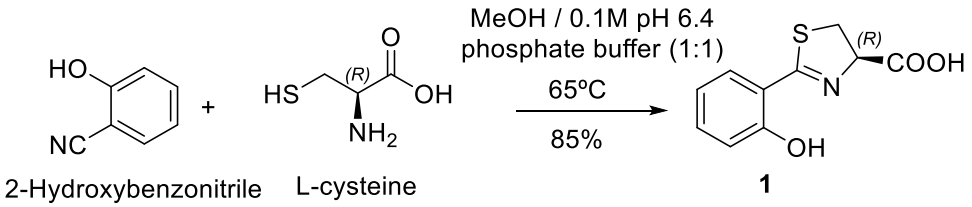

*Scheme 2. Synthesis of compound **1**.*

The synthesis of fragment A *(Scheme 3)* started with the protection of the carboxylic acid of compound **1**. For this purpose, it was protected as a methyl ester using H_2SO_4 in MeOH at 65 °C to give **2** *(Scheme 4)*.[22] The formation was confirmed both by analysis of its ^{1}H NMR spectrum and by its high-resolution mass spectrum.

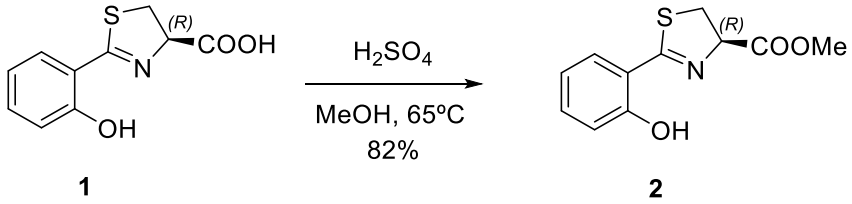

*Scheme 3. Synthesis of compound **2**.*

After esterification of **1**, **2** was oxidized with bromotrichloromethane ($BrCCl_3$) and DBU in CH_2Cl_2 at -20°C to form the thiazole **3** *(Scheme 4).*[22] The most characteristic signal was the thiazole proton observed as a singlet at 8.11 ppm in the ^{1}H-NMR spectrum of **3**, which along with its high-resolution mass spectrum confirmed its formation.

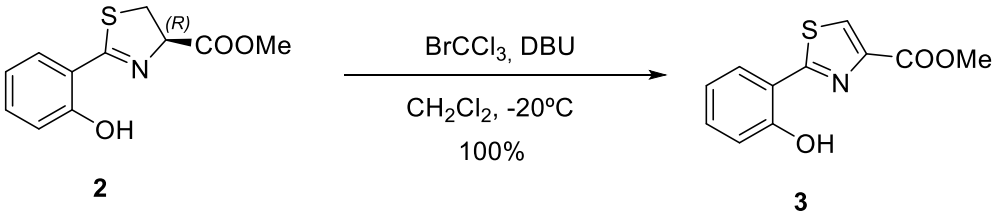

*Scheme 4. Synthesis of compound **3**.*

Then, the OH of compound **3** was protected with the isopropyl group (^{i}Pr), due to its robust character under different reaction conditions. Isopropylation was achieved by adding ^{i}PrBr and KI, in the presence of the base K_2CO_3 in DMF at 60 °C. The methyl ester of **4** was then hydrolyzed with $Ba(OH)_2$ *(Scheme 5).*[22]

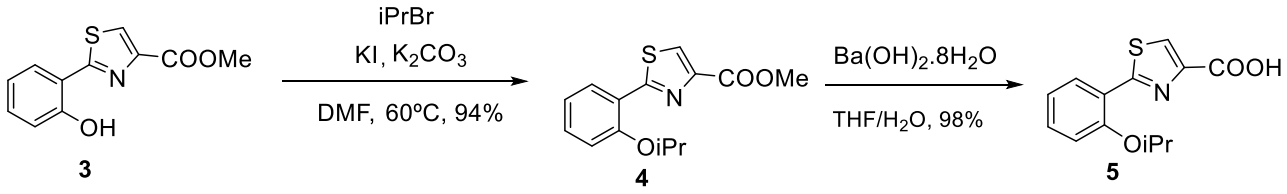

*Scheme 5. Synthesis of compound **4** and **5**.*

In the ^{1}H-NMR spectra of compounds **4** and **5**, signals corresponding to the ^{i}Pr group are observed at 4.47 and 1.52 ppm *(Figure 8).* The formation of both compounds was also confirmed by mass spectrometry.

1)

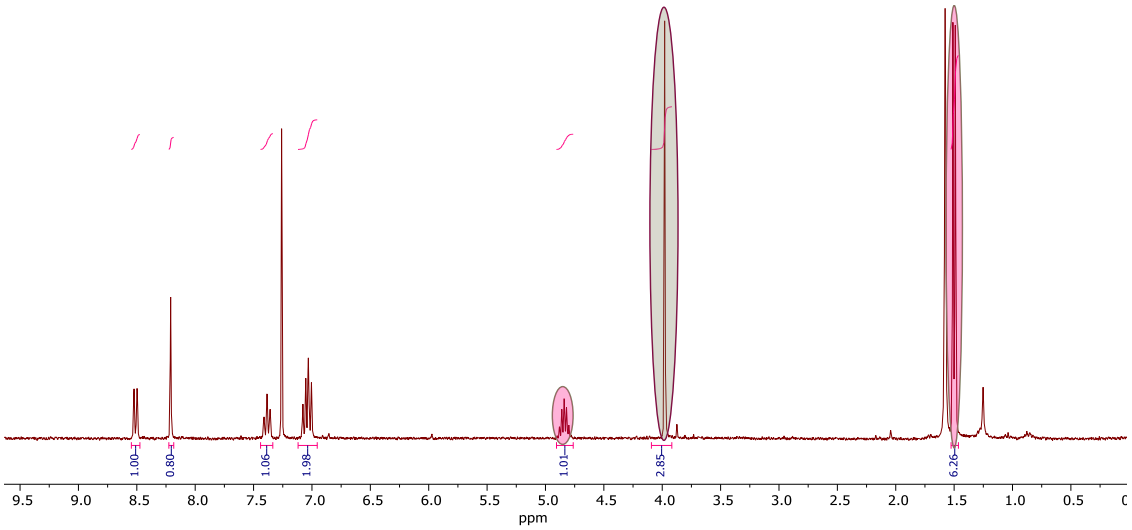

2)

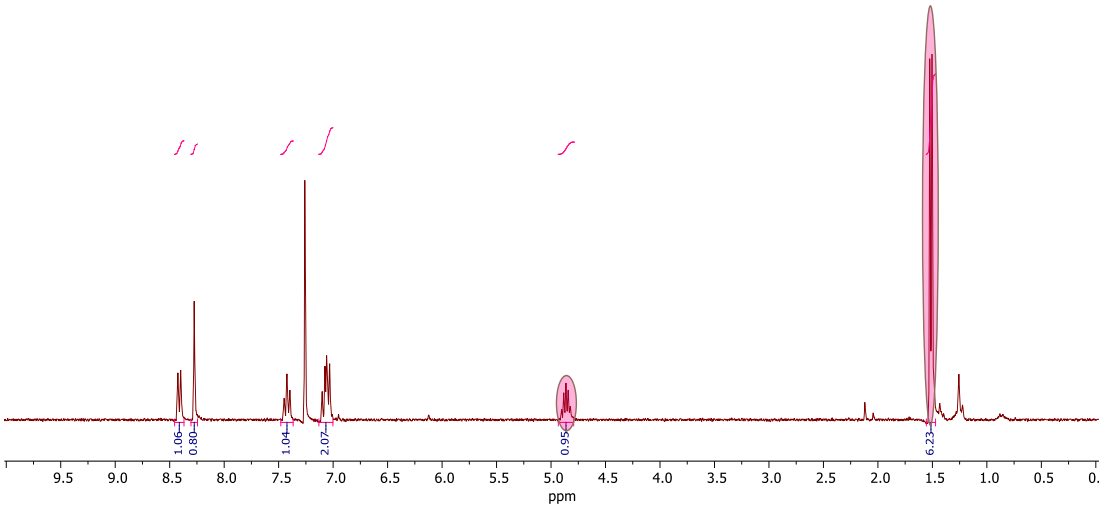

*Figure 8. ^{1}H-NMR spectra: **1)** compound **4**; **2)** compound **5**. The most relevant signals are coloured.*

For the conjugation of compound **5** with D-serine methyl ester the coupling agent TBTU and Et_3N as a base in DMF were used *(Scheme 6).*[22] In addition, the protection of the phenolic OH accelerates the reaction.

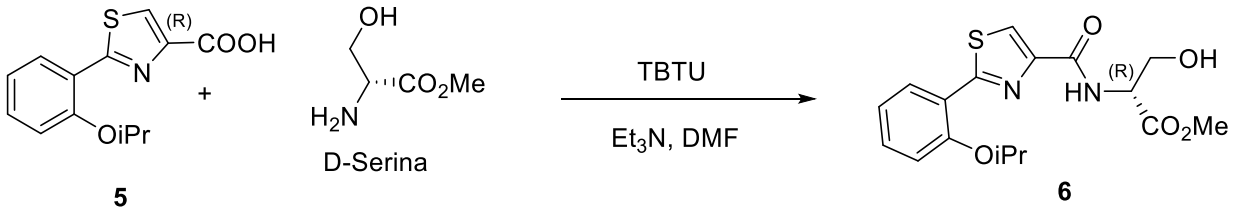

5 **6**

*Scheme 6. Synthesis of compound **6**.*

4 EXPERIMENTAL PROCEDURE

4.1 General Methods

All moisture-sensitive reactions were carried out under an atmosphere of dry deoxygenation argon (Ar C-50) in dried glassware, closed by rubber septum. The dry solvent CH_2Cl_2 was obtained by pre-drying and refluxing it over calcium hydride (CaH_2), while DMF and Et_3N used a commercial version of 99.8% extra dry purity, AcroSealTM from ACROS OrganicsTM. The rest of the solvents and reagents were used unpurified. Anhydrous solvents (DMF, MeOH and Et_3N) were purchased from commercial sources. Solutions and solvents were added via syringe.

Cryocool-immersion CC-100 II (Neslab) in a bath of acetone was used for low temperature reactions. When necessary, reactions were heated using a stir plate equipped with an aluminium heating block.

The reference method for follow-up the reactions, the thin-layer chromatography (TLC), was performed using silica gel GF-254 Merck and spots were revealed employing UV light (λ =254 nm).

The Nuclear Magnetic Resonance characterization were recorded on Bruker AVANCE 300 spectrometer, with a NEO console (300 MHz for ^{1}H and 75 MHz for ^{13}C) of the CICA (Interdisciplinary Center for Chemistry and Biology) using $CDCl_3$ (99.8% D) as the solvent. The electrospray mass spectra (ESI) were performed on a ThermoLTQ Orbitrap Discovery mass spectrometer of the SAI (Research Support Service of the University of A Coruña).

4.2 Procedure and characterization

4.2.1 SYNTHESIS OF 1

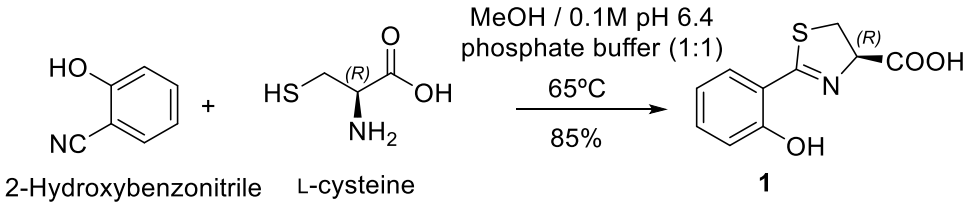

2-Hydroxybenzonitrile (51 mg, 427,29 µmol) was dissolved in 10 mL mixture of MeOH/0.1M pH 6.4 phosphate buffer (1:1) and L-cysteine (102.9 mg, 849.33 µmol) were added. To accelerate the dissolution, ultrasonic method was used. The pH of the reaction was kept at 6.4 and stirred at 65 °C overnight. The solvent was concentrated in vacuum; the residue was dissolved in water (10 mL) and the solution was adjusted to pH 2-3 by the addition of 5% HCl. The aqueous layer was extracted with CH_2Cl_2 (3 × 20 mL), the organic layers were collected, pre-dried by Mg_2SO_4 and filtered. The solvent was removed under reduced pressure to give the thiazoline **1** as a brown foam (81 mg, 85 %). **^{1}H-NMR (300 MHz, $CDCl_3$) δ ppm** 7.45-7.35 (m, 2H, H3, H5), 7.02 (d, J = 7.7 Hz, 1H, H6), 6.89 (t, J = 7.7 Hz, 1H, H4), 5.41 (t, J = 9.0 Hz, 1H, H9), 3.66 (q, J = 9.0 Hz, 2H, H8). **^{13}C NMR (75 MHz, $CDCl_3$) δ ppm** 175.11 (COOH, C10), 172.82 (C, C7), 158.8 (C, C1), 133.94 (CH, C5), 130.99 (C, C3), 119.25 (CH, C4), 117.54 (CH, C6), 115.97 (C, C2), 76.44 (CH, C9), 33.77 (CH_2, C8). **(+)-HRMS (ESI) *m/z:*** 224.0376 $[M+H]^+$ (calculated to $C_{10}H_{10}NO_3S^+$: 224.0376)

4.2.2 SYNTHESIS OF 2

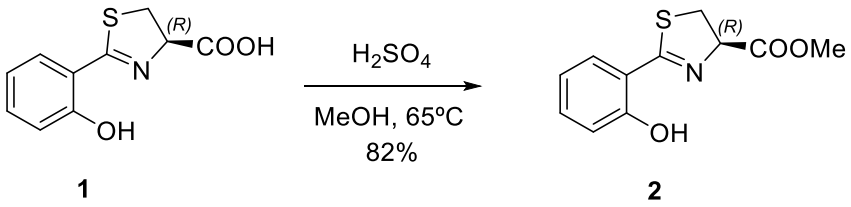

Over the solution of **1** (230 mg, 1.03 mmol) in MeOH (10 mL), H_2SO_4 90-91% (81 µL, 1,49 mmol) were added and stirred at reflux overnight (65 °C). After that time, the reaction was left to reach room temperature and the resulting solution was neutralize with K_2CO_3, filtered and concentrated under reduced pressure. The residue was redissolved in EtOAc (10 mL) and H_2O (10 mL). Once the phases were separated, the aqueous phase was washed with EtOAc. The combined organic phases were washed with brine, pre-dried with

Mg_2SO_4, and filtered. The solvent was evaporated under reduced pressure to give **2** as a brown oil (200 mg, 82%) **^{1}H NMR (300 MHz, $CDCl_3$) δ ppm** 7.47 – 7.36 (m, 2H, H3-H5), 7.04 (d, J = 8.4 Hz, 1H, H6), 6.91 (t, J = 7.6 Hz, 1H, H4), 5.37 (t, 1H, H9), 3.85 (s, 3H, H11), 3.77 – 3.56 (m, 2H, H8). **^{13}C NMR (75 MHz, $CDCl_3$) δ ppm** 174.51 ($COOMe_1$, C10), 170.82 C, C7), 159.28 (C, C1), 133.73 (CH, C5), 130.94 (CH, C3), 119.14 (CH, C4), 117.43 (CH, C6), 116.13 (C, C2), 76.86 (CH, C9), 53.05 (CH_3, C11), 33.84 (CH_2, C8). **(+)-HRMS (ESI)** ***m/z:*** 260.0352 $[M+Na]^+$ (calculated to $C_{11}H_{11}NNaO_3S^+$: 260.0352)

4.2.3. SYNTHESIS OF 3

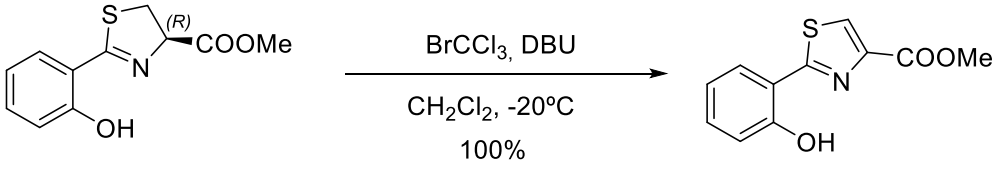

2 **3**

To a solution of **2** (200 mg, 0.84 mmol) in dry CH_2Cl_2 (10 mL) was added DBU (214 µL, 1.69 mmol) and the resulting solution was stirred at –20 °C. After 5 min, $BrCCl_3$ (133 µL, 1.35 mmol) was added. The solution was warmed up slowly and stirred during 2 h under inert atmosphere. After this time, all of the starting material was consumed. The reaction mixture was washed with 10 mL $NaHCO_3$ saturated solution, water, 0.05 M HCl, water and brine. The organic phase was pre-dried with Mg_2SO_4, filtered and concentrated under vacuum to give **4** as a white solid (quantitative yield). **^{1}H NMR (300 MHz, $CDCl_3$) δ ppm** 8.11 (s, 1H, H8), 7.62 (d, J = 7.9 Hz, 1H, H3), 7.36 (t, J = 7.8 Hz, 1H, H5), 7.09 (d, J = 8.2 Hz, 1H, H6), 6.93 (t, J = 7.4 Hz, 1H, H4), 3.97 (s, 3H, H11), **^{13}C NMR (75 MHz, $CDCl_3$) δ ppm** 166.99 (COOMe, C10), 161.03 (C, C7),157.05 (C, C1), 145.72 (C, C9), 132.58 (CH, C5), 127.36 (CH, C3), 125.25 (CH, C8), 119.57 (CH, C4), 118.16 (CH, C6), 116.25 (C, C2), 52.53 (CH_3, C11). **(+)-HRMS (ESI)** ***m/z:*** 258.0196 $[M+Na]^+$ (calculated to $C_{11}H_9NNaO_3S^+$: 258.0195)

4.2.4. SYNTHESIS OF 4

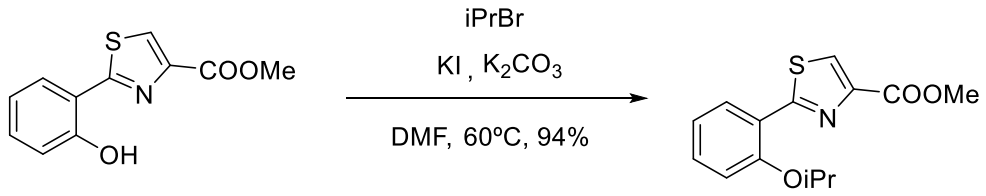

3 **4**

Compound **3** (199 mg, 0.86 mmol) in presence of KI (508 mg, 3.06 mmol), K_2CO_3 (467 mg, 3.38 mmol) were solved in 4 mL anhydrous DMF. Isopropyl bromide (^{i}PrBr) (160 µL, 1,69 mmol) was added. The solution was stirred at 60 ºC under inert atmosphere for 2 h. Then, the reaction was left to reach room temperature and it was concentrated by rotavapor. It was distributed in CH_2Cl_2 (10 mL) y H_2O (10 mL), and the phases were separated. The organic phase was washed with 5% HCl (10 mL) and brine (10 mL). Finally was pre-dried with Mg_2SO_4, filtered and concentrated in vacuum to obtain **4** as yellow oil (220 mg, 94%) **^{1}H NMR (300 MHz, $CDCl_3$) δ ppm** 8.51 (d, J = 7.9Hz, 1H, H3), 8.21 (s, 1H, H8), 7.39 (t, J = 7.9Hz, 1H, H5), 7.05-7.00 (m, 2H, H4-H6), 4.84 (hept, J = 6.1 Hz, 1H, ^{i}Pr), 3.98 (s, 3H, H11), 1.50 (d, J = 6.1 Hz, 6H, ^{i}Pr) **^{13}C NMR (75 MHz, $CDCl_3$) δ ppm** 168.08 (COOMe, C10), 163.60 (C, C7), 161.82 (C, C1), 154.98 (C, C9), 131.33 (CH, C5), 129.39 (CH, C3), 128.19 (CH, C8), 122.40 (C, C2), 120.85 (CH, C4), 113.07 (CH, C6), 71.82 (CH, ^{i}Pr), 52.51 (CH3, C11), 22.36 (CH_3, ^{i}Pr)**. (+)-HRMS (ESI)** ***m/z:*** 300.0667 $[M+Na]^+$ (calculated to $C_{14}H_{15}NO_3S^+$: 300.0665)

4.2.5. SYNTHESIS OF 5

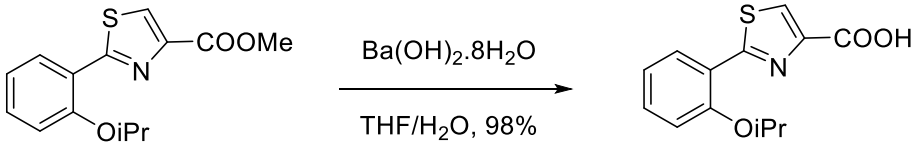

4 **5**

A solution of **4** (33 mg, 0.12 mmol) in a THF/H_2O mixture 1:1 (6 mL) was stirred in presence of the base $Ba(OH)_2{\cdot}8H_2O$ (56 mg, 0.18 mmol) at room temperature for 3 h. After that time, THF was evaporated, and the resulting aqueous solution was redissolved in 10 mL of EtOAc and acidificated with 5% HCl. The phases were separated, and the aqueous one was extracted with EtOAc (2 x 10 mL). The combined organic phases were pre-drying with Mg_2SO_4, filtered, and concentrated under reduce pressure to give **5** as yellow dough (30 mg, 98%). **^{1}H NMR (300 MHz, $CDCl_3$) δ ppm** 8.41 (d, J = 7.9 Hz, 1H, H3), 8.27 (s, 1H, H8), 7.42 (t, J = 7.9 Hz, 1H, H5), 7.07 (dd, J = 7.9 Hz, 2H, H4, H6), 4.86

(hept, J = 6.2 Hz, 1H, ^{i}Pr), 1.51 (d, J = 6.2 Hz, 6H, ^{i}Pr) **^{13}C NMR (75 MHz, $CDCl_3$) δ ppm** 161.79 (COOH, C10), 155.00 (C, C7), 144.60 (C, C1), 133.12 (C, C9), 131.67 (CH, C5), 128.75 (CH, C3), 127.69 (CH, C8), 123.64 (C, C2), 120.78 (CH, C4), 113.08 (CH, C6), 71.85 (CH, ^{i}Pr), 22.20 (CH_3, ^{i}Pr). **(+)-HRMS (ESI) *m/z:*** 286.0509 $[M+Na]^+$ (calculated to $C_{13}H_{13}NNaO_3S^+$: 286.0508).

4.2.6. SYNTHESIS OF 6

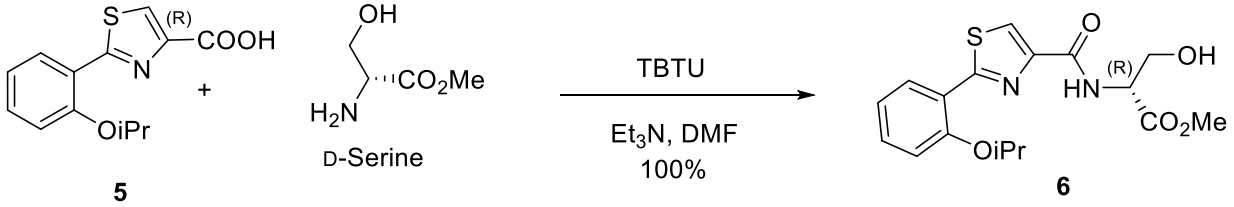

5 **6**

To a solution of compound **5** (77 mg, 0.29 mmol) in 2 mL DMF, D-Seryne (48 mg, 0.31 mmol), TBTU (86 mg, 0.27 mmol) and Et_3N (100 µL, 0.72 mmol) was added. It was stirred 3 h under inert atmosphere. Then, the solution was concentrated in a rotavapor and redissolved in 10 mL of EtOAc and washed with $NaHCO_3$ saturated, water, 0.05 M HCl and NaCl brine (saturated). It was pre-dried with Mg_2SO_4, filtered, and used the rotavapor again to give **6** as yellow solid (quantitative yield). **^{1}H NMR (300 MHz, $CDCl_3$) δ ppm** 8.48 (d, J = 7.8 Hz, 1H, H3), 8.37 (d, J = 7.5 Hz, 1H, NH), 8.18 (s, 1H, H8), 7.41 (t, J = 9.6 Hz, 1H, H5), 7.15 – 7.01 (m, 2H, H4-H6), 4.97 – 4.80 (m, 2H, ^{i}Pr-H11), 4.13 (d, J = 3.8 Hz, 2H, H12), 3.87 (s, 3H, H14),1.52 (d, J = 9.45, 6H, ^{i}Pr) **^{13}C NMR (75 MHz, $CDCl_3$) δ ppm** 170.81 (COOMe, C13), 163,94 (C, C7), 162.02 (C, C10), 154.94 (C, C1), 147.71 (C, C9), 131.17 (CH, C5), 128.75 (CH, C3), 124.48 (CH, C8), 122.22 (C, C2), 120.72 (CH, C4), 113.11 (CH, C6), 71.72 (CH, ^{i}Pr), 63.81 (CH2, C12), 55.01 (CH, C11), 52.84 (CH_3, C14), 22.19 (CH_3, ^{i}Pr). **(+)-HRMS (ESI) m/z:** 387.0976 $[M+Na]^+$ (calcd. para $C_{17}H_{20}N_2NaO_5S^+$: 387.0985).

5 CONCLUSIONS

The following conclusions were decided from the obtained results:

- The preparation of an advanced intermediate for the synthesis of a simplified Pcb analogue was achieved, which can be used in future projects.
- The structures of all synthesized compounds were confirmed by analysis of the corresponding ^{1}H-NMR and ^{13}C-NMR and high-resolution mass spectra.

6 CONCLUSIONES

De los resultados obtenidos se deducen las siguientes conclusiones:

- Se logró la preparación de un intermedio avanzado de la síntesis de un análogo simplificado de Pcb, que podría ser usado en las próximas elaboraciones en futuros proyectos.
- Las estructuras de todos los compuestos sintetizados se confirmaron mediante el análisis de los correspondientes espectros de ^{1}H-NMR y ^{13}C-NMR y de masas de alta resolución.

7 CONCLUSIÓNS

Dos resultados obtidos pódense extraer as seguintes conclusións:

- Logrouse a preparación dun intermediario avanzado na síntese dun análogo simplificado de Pcb, que podería ser empregado nas próximas elaboracións en proxectos futuros.
- A estructura de todolos compoñentes sintetizados confirmouse mediante o análise dos correspondentes espectros de ^{1}H-NMR e ^{13}C-NMR e de masas de alta resolución.

8 REFERENCES

(1) World Health Organization: WHO. (2022, 7 julio). *Peste*. https://www.who.int/es/news-room/fact-sheets/detail/plague (accessed 3 Dec. 2024)

(2) *Ecology and transmission of plague | CDC*. (2019, 31 julio). Centers For Disease Control And Prevention. https://www.cdc.gov/plague/transmission/index.html (accessed 3 Jan. 2024)

(3) Bush, L. M., & Vazquez-Pertejo, M. T. (2023, 15 noviembre). *Peste y otras infecciones por Yersinia.* Manual MSD Versión Para Profesionales. https://www.msdmanuals.com/es-es/professional/enfermedades-infecciosas/bacilos-gramnegativos/peste-y-otras-infecciones-por-yersinia (accessed 3 Jan. 2024)

(4) BBC News Mundo. (2020, 11 agosto). Qué es la peste negra (o peste bubónica) y por qué a pesar de que haya brotes como el de China ya no es tan mortal. *BBC News Mundo*. https://www.bbc.com/mundo/noticias-53739596#:~:text=%C2%BFQu%C3%A9%20es%20la%20peste%20bub%C3%B3nica%3F,llevan%20estos%20en%20su%20pelaje (accessed 3 Jan. 2024)

(5) Professional, C. C. M. (s. f.). *Bubonic Plague*. Cleveland Clinic. https://my.clevelandclinic.org/health/diseases/21590-bubonic-plague (accessed 9 Feb. 2024)

(6) Seven, J. (2023, 16 mayo). *The Black Death: A Timeline of the Gruesome Pandemic*. HISTORY. https://www.history.com/news/black-death-timeline (accessed 3 Dec. 2024)

(7) Luaces, P. G. (2019, 12 septiembre). La gran epidemia medieval. *La Vanguardia.* https://www.lavanguardia.com/historiayvida/edad-media/20170306/47310452522/la-gran-epidemia-medieval.html#:~:text=La%20peste%20negra%20contribuy%C3%B3%20a,transformar%C3%ADa%20radicalmente%20al%20hombre%20medieval.&text=Per%C3%ADodo%20un%20tanto%20imprec (accessed 6 Dec. 2024)

(8) *PressReader.com - digital newspaper & magazine subscriptions.* (s. f.). PressReader. https://www.pressreader.com/spain/muy-historia/20131025/282054799773614

(9) Sancristán, E. (2022). *La peste negra se originó en el corazón de Asia*. https://www.agenciasinc.es/Noticias/La-peste-negra-se-origino-en-el-corazon-de-Asia (accessed 4 Jan. 2024)

(10) Jiménez, J. (2023, 11 agosto). *Acabamos de resolver el mayor misterio de la historia de la medicina: el lugar donde empezó la peste*.Xataka. https://www.xataka.com/medicina-y-salud/acabamos-resolver-mayor-misterio-historia-medicina-lugar-donde-empezo-peste-negra-1 (accessed 4 Jan. 2024)

(11) Tomás Cabot, J. (1974). *La última batalla contra la Peste* (pp. 52–57)

(12) *Plague surveillance* | CDC. (2022, 16 noviembre). Centers For Disease Control And Prevention. https://www.cdc.gov/plague/maps/index.html (accessed 3 Jan. 2024)

(13) BBC News. (2020, 7 julio). China bubonic plague: WHO «monitoring» case but says it is «not high risk». *BBC News*. https://www.bbc.com/news/world-asia-china-53325988 (accessed 5 Jan. 2024)

(14) *AMR Action plan 2017 Factsheet.* (2017). https://health.ec.europa.eu/system/files/2020-01/amr_2017_factsheet_0.pdf

(15) *AMR Action plan 2017.* (2017). https://health.ec.europa.eu/system/files/2020-01/amr_2017_action-plan_0.pdf

(16) Rodríguez, H. (2022, 3 abril). En 2050 la resistencia a los antibióticos será responsable de 10 millones de muertes anuales. *www.nationalgeographic.com.es.* https://www.nationalgeographic.com.es/ciencia/2050-resistencia-a-antibioticos-sera-responsable-10-millones-muertes-anuales_18090 (accessed 6 Dec. 2024)

(17) Antimicrobial resistance: a global threat. (s. f.). UNEP - UN Environment Programme. https://www.unep.org/topics/chemicals-and-pollution-action/pollution-and-health/antimicrobial-resistance-global-threat (accessed 25 Jan. 2024)

(18) *Preguntas y respuestas sobre la resistencia a los antibióticos.* (2020 julio). https://www.cdc.gov/antibiotic-use/sp/antibiotic-resistance.html (accessed 25 Jan. 2024)

(19) D. Wright, G. (2011). Molecular mechanisms of antibiotic resistance (p. 1). *Chem. Commun., 2011,47, 4055-4061* https://doi.org/10.1039/C0CC05111J

(20) R. D. Perry, A. Bobrov and J. D. Fetherston (2015), The Role of Transition Metal Transporters for Iron, Zinc, Manganese, and Copper in the Pathogenesis of Yersinia pestis, *Metallomics*, 10.1039/C4MT00332B.

(21) Hierro. (2024, 2 enero). Linus Pauling Institute. https://lpi.oregonstate.edu/es/mic/minerales/hierro (accessed 25 Jan. 2024)

(22) Rodríguez Pedrouzo, A. (2023). Aproximación sintética de análogos estables del sideróforo Piscibactina [Traballo de fin de mestrado, Universidade da Coruña. Facultade de Ciencias]. http://hdl.handle.net/2183/33407

(23) Freddy Rivault, Viviane Schons, Clémence Liébert, Alain Burger, Elias Sakr, Mohamed A. Abdallah, Isabelle J. Schalk, Gaëtan L.A. Mislin (2006), Synthesis of functionalized analogs of pyochelin, a siderophore of Pseudomonas aeruginosa and Burkholderia cepacian, *Tetrahedron*, *62* (10), 2247-2254, https://doi.org/10.1016/j.tet.2005.12.012.

(24) Hider, R. C.; Kong (2010), X. Chemistry and Biology of Siderophores, *Nat Prod Rep, 27* (5), 637–657. https://doi.org/10.1039/b906679a.

(25) Holden, V.I., & Bachman, M.A. (2015). Diverging roles of bacterial siderophores during infection. *Metallomics: integrated biometal science, 7 6*, 986-95. https://doi.org/10.1039/c4mt00333k

(26) Diana Rodríguez, Concepción González-Bello (2023), Siderophores: Chemical tools for precise antibiotic delivery, *Bioorganic & Medicinal Chemistry Letters*, 87, https://doi.org/10.1016/j.bmcl.2023.129282.

(27) Ratledge, C.; Dover, L. G. (2000), Iron Metabolism in Pathogenic Bacteria. *Annu Rev Microbiol*, 54, 881–941. https://doi.org/10.1146/annurev.micro.54.1.881

(28) M. Carmen de la Fuente, Lucía Ageitos, Marta A. Lages, Diana Martínez-Matamoros, Abel M. Forero, Miguel Balado, Manuel L. Lemos, Jaime Rodríguez, and Carlos Jiménez (2023), Structural Requirements for Ga3+ Coordination in Synthetic Analogues of the Siderophore Piscibactin Deduced by Chemical Synthesis and Density Functional Theory Calculations, *Inorganic Chemistry,* 62 (19), 7503-7514 https://doi.org/10.1021/acs.inorgchem.3c00787

(29) M. Carmen de la Fuente, Yuri Segade, Katherine Valderrama, Jaime Rodríguez, and Carlos Jiménez (2021), Convergent Total Synthesis of the Siderophore Piscibactin as Its Ga3+ Complex, *Organic Letters 23* (2), 340-345 https://dx.doi.org/10.1021/acs.orglett.0c03850

(30) Menna-Allah W. Shalaby, Eman M.E. Dokla, Rabah.A.T. Serya, Khaled A.M. Abouzid (2020), Penicillin binding protein 2a: An overview and a medicinal chemistry perspective, European Journal of Medicinal Chemistry, 199, https://doi.org/10.1016/j.ejmech.2020.112312

(31) Shabnam Sharifzadeh, Nathaniel W. Brown, Joshua D. Shirley, Kevin E. Bruce, Malcolm E. Winkler, Erin E. Carlson (2020), Chapter Two - Chemical tools for selective activity profiling of bacterial penicillin-binding proteins, Methods in Enzymology, 638, (27-55), https://doi.org/10.1016/bs.mie.2020.02.015

(32) Soriano, M. C., Montufar, J., & Blandino-Ortiz, A. (2022). Cefiderocol. Revista espanola de quimioterapia : publicacion oficial de la Sociedad Espanola de Quimioterapia, 35 Suppl 1(Suppl 1), 31–34. https://doi.org/10.37201/req/s01.07.2022

(33) Wang H, Palasik BN (2022), Combating antimicrobial resistance with cefiderocol for complicated infections involving the urinary tract, *Therapeutic Advances in Urology*; 14 https://doi.org/10.1177/17562872211065570

(34) Hu, X., Feng, J., Zhou, Q., Luo, L., Meng, T., Zhong, Y., Tang, W., Deng, S., & Li, X. (2019). Respiratory Syncytial Virus Exacerbates Kidney Damages in IgA Nephropathy Mice via the C5a-C5aR1 Axis Orchestrating Th17 Cell Responses. Frontiers in cellular and infection microbiology, 9, 151. https://doi.org/10.3389/fcimb.2019.00151

(35) European Food Safety Authority. (2009, November 11). EFSA reports aim to harmonise monitoring of two food-borne zoonoses. European Food Safety Authority. https://www.efsa.europa.eu/en/press/news/091111#links-to-science (accessed 8 Feb. 2024)

(36) Gomez, V. (2022, June 14). *Yersinia enterocolitica.* Lifeder. https://www.lifeder.com/yersinia-enterocolitica/ (accessed 8 Feb. 2024)

(37) Martínez, P. (2022, September 29). La Yersinia enterocolitica. *Pascual Martínez.* https://www.lasendanatural.com/yersinia/ (accessed 8 Feb. 2024)

(38) Robert D. Perry, Jacqueline D. Fetherston (2011), Yersiniabactin iron uptake: mechanisms and role in Yersinia pestis pathogenesis, *Microbes and Infection, 13 (*10), 808-817, https://doi.org/10.1016/j.micinf.2011.04.008

(39) Ino, Akira and Murabayashi, Akira (2001), Synthetic studies of thiazoline and thiazolidine-containing natural products. Part 3: Total synthesis and absolute configuration of the siderophore yersiniabactin, *Tetrahedron,* 57, 1897-1902, https://doi.org/10.1016/S0040-4020(01)00012-6

9 APPENDIX

^{1}H-NMR (300 MHz, $CDCl_3$) of **1**

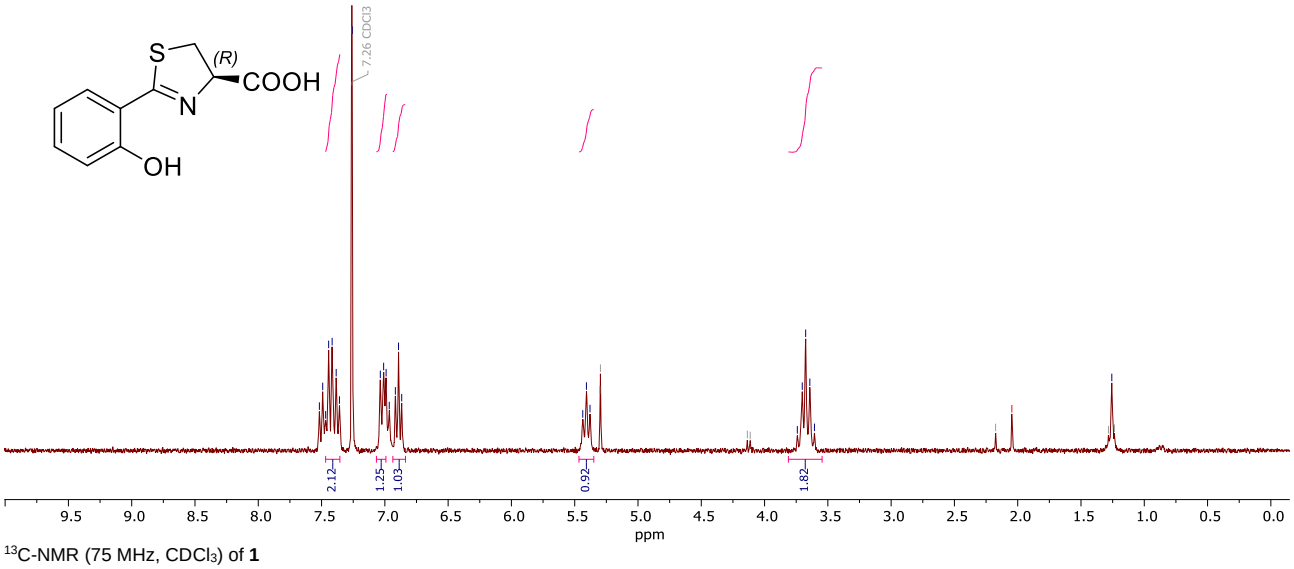

^{13}C-NMR (75 MHz, $CDCl_3$) of **1**

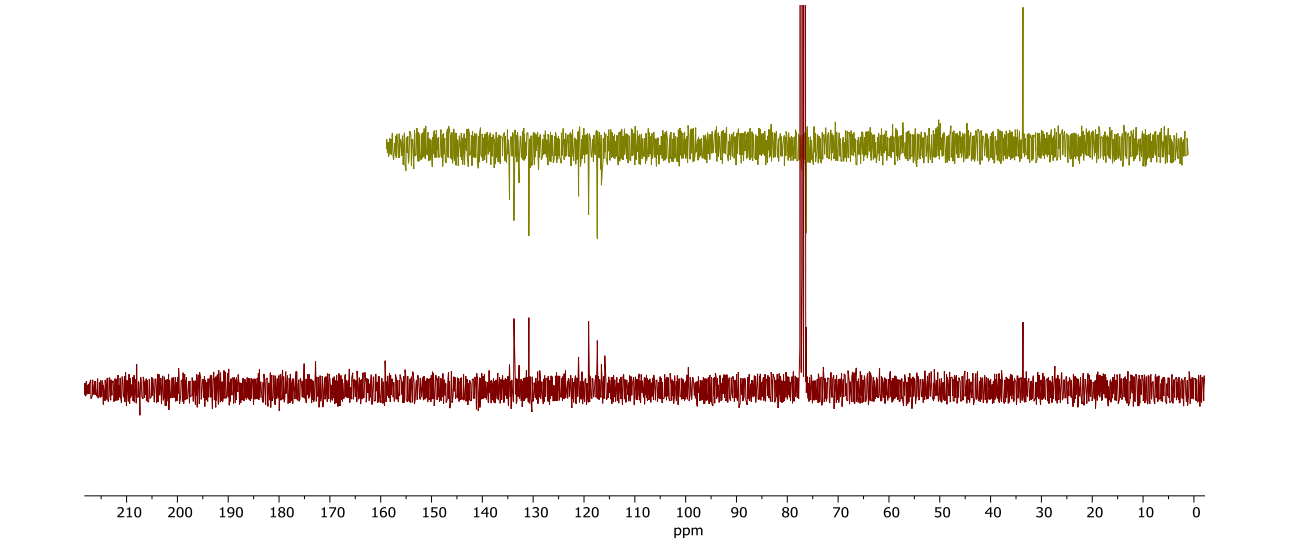

(+)- HRMS (ESI) of **1**

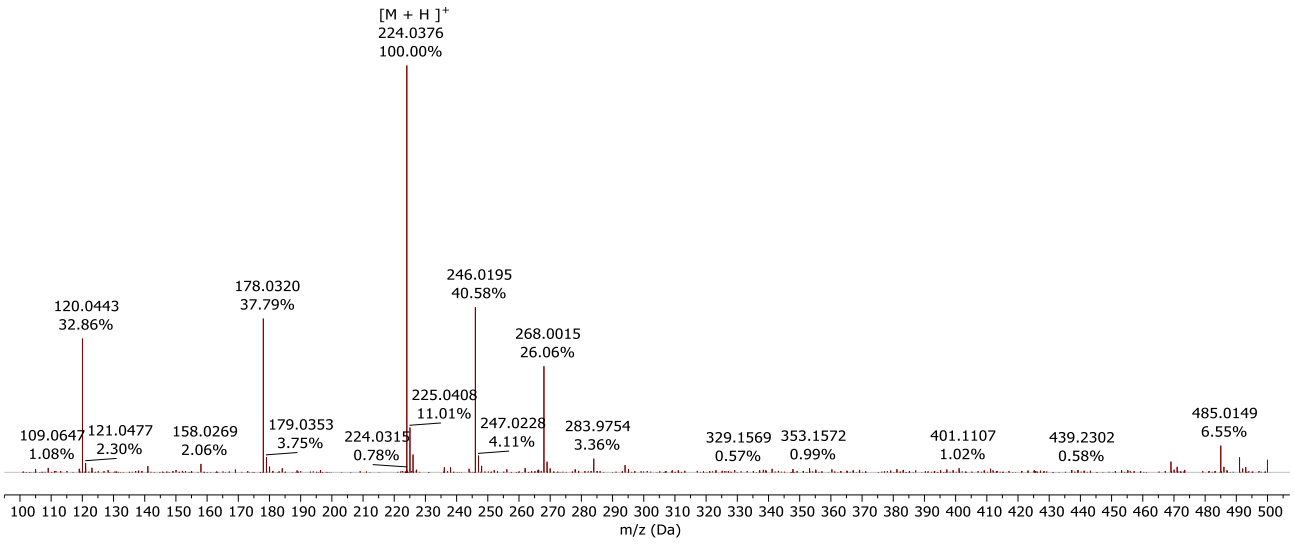

^{1}H-NMR (300 MHz, $CDCl_3$) of **2**

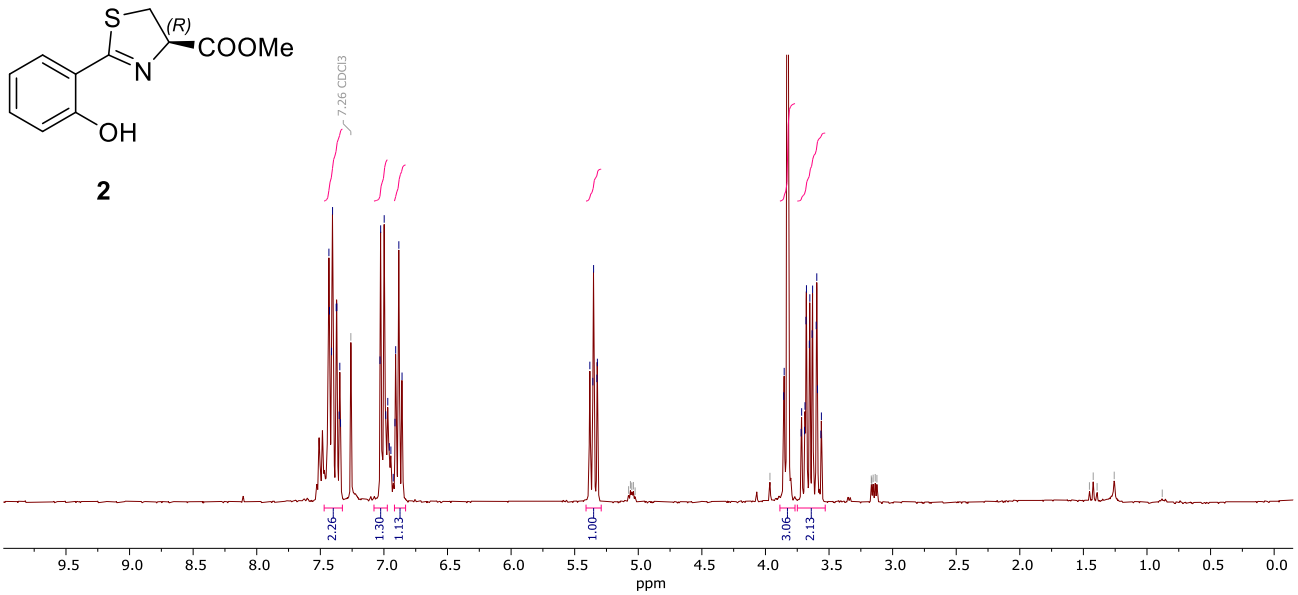

2

^{13}C-NMR (75 MHz, $CDCl_3$) of **2**

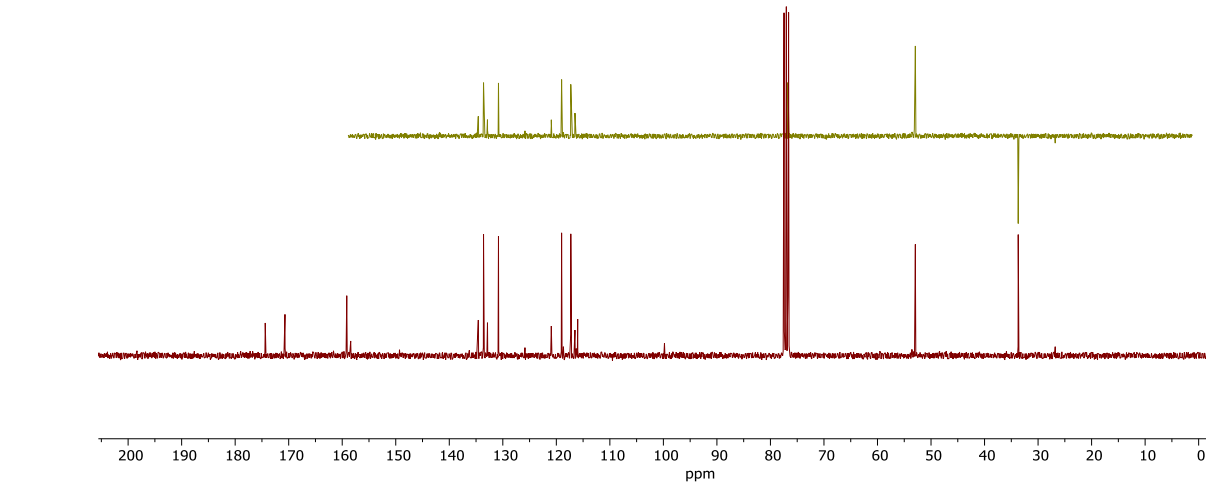

(+)- HRMS (ESI) of **2**

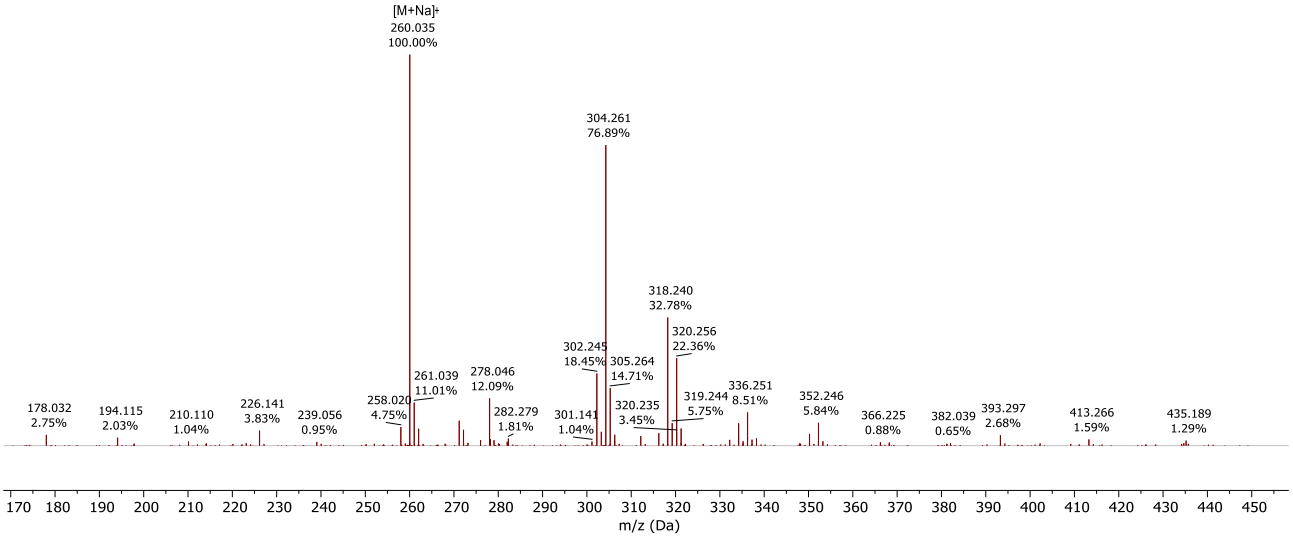

^{1}H-NMR (300 MHz, $CDCl_3$) of **3**

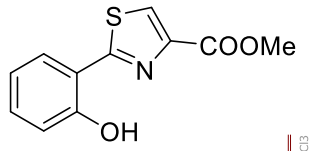

3

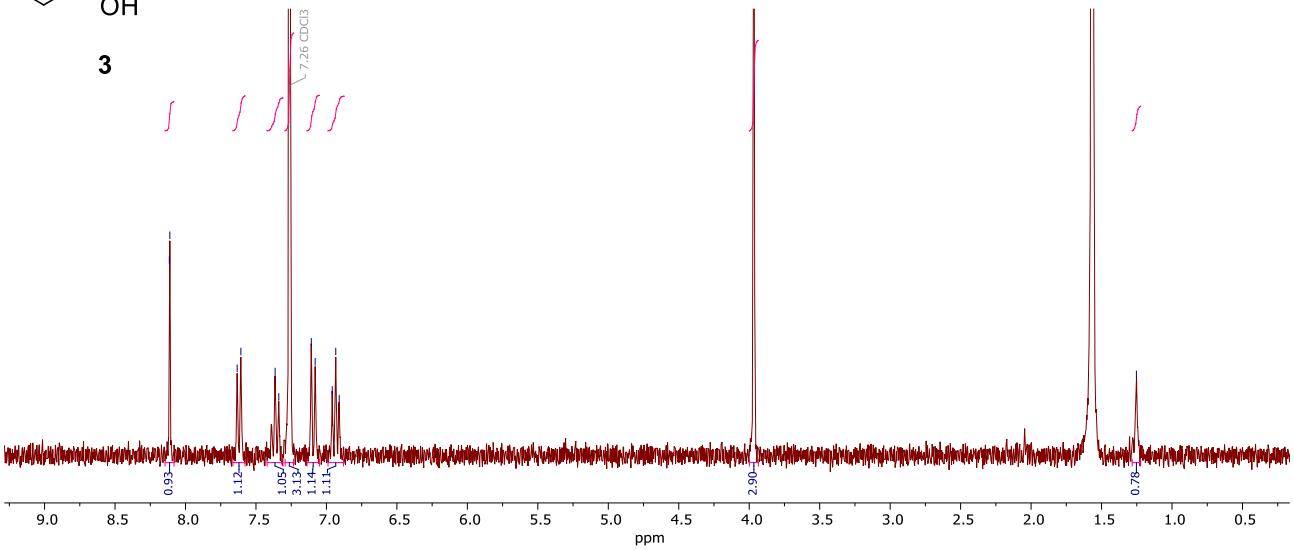

^{13}C-NMR (75 MHz, $CDCl_3$) of **3**

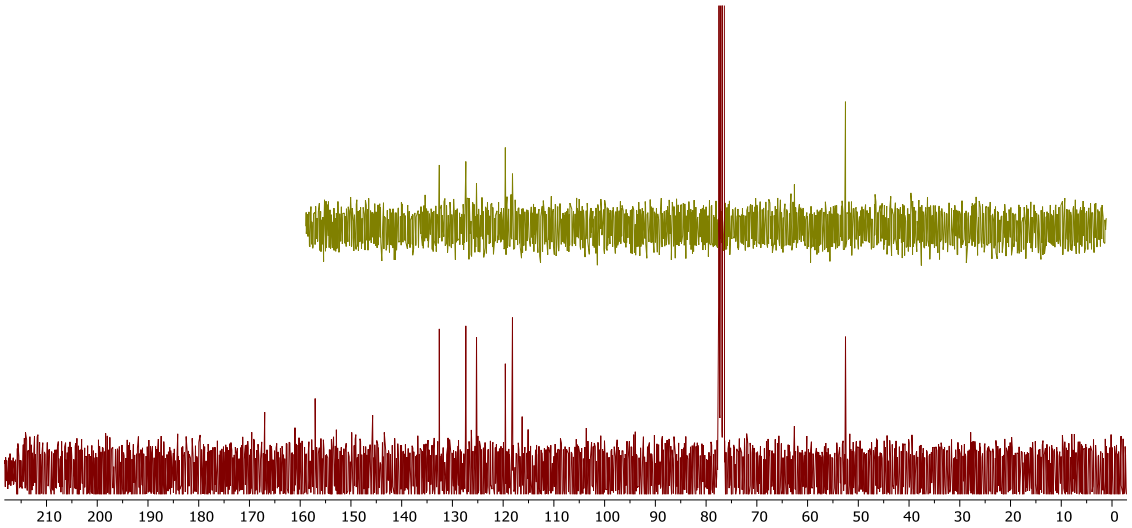

(+)- HRMS (ESI) of **3**

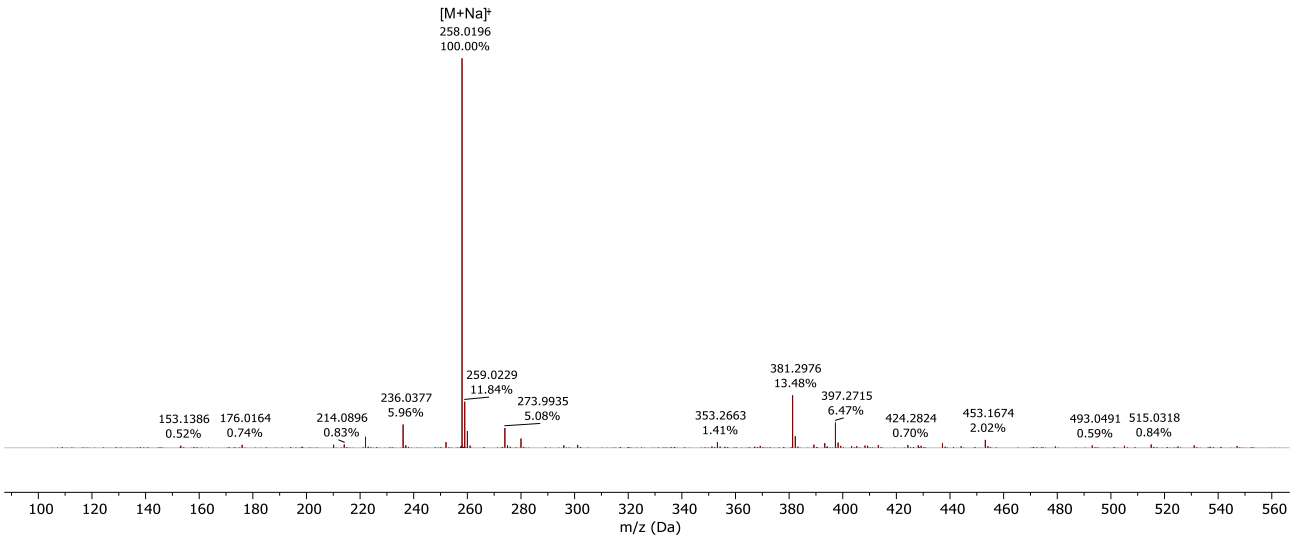

^{1}H-NMR (300 MHz, $CDCl_3$) of **4**

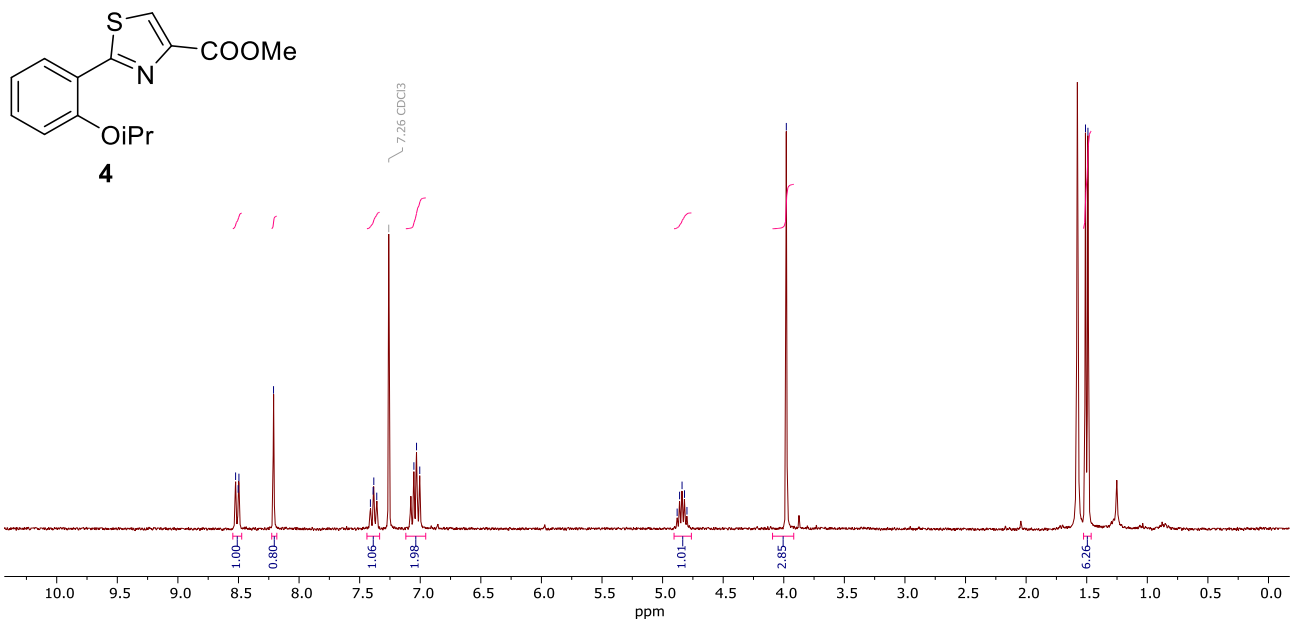

^{13}C-NMR (75 MHz, $CDCl_3$) of **4**

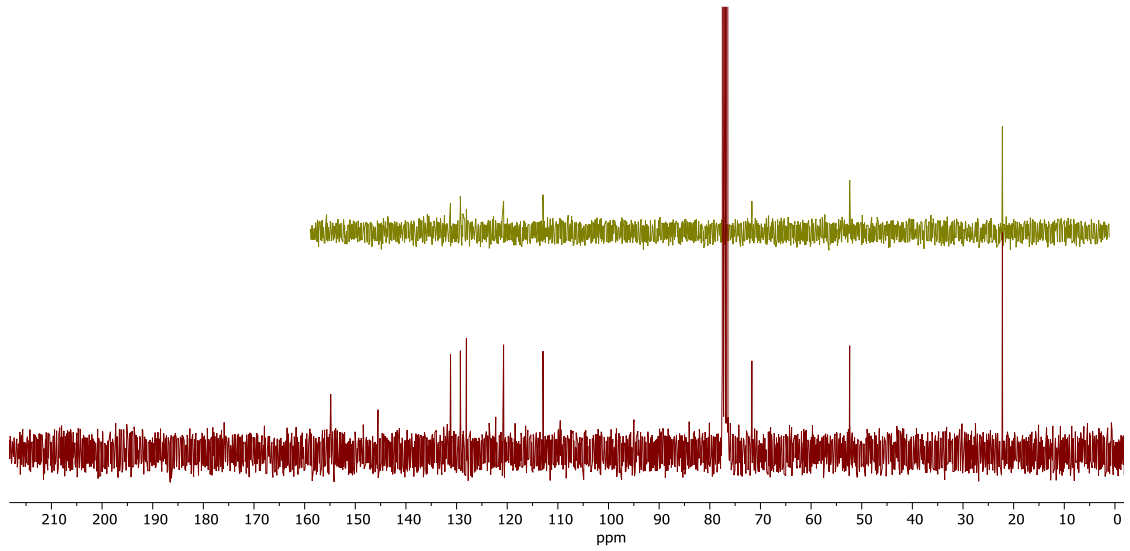

(+)- HRMS (ESI) of **4**

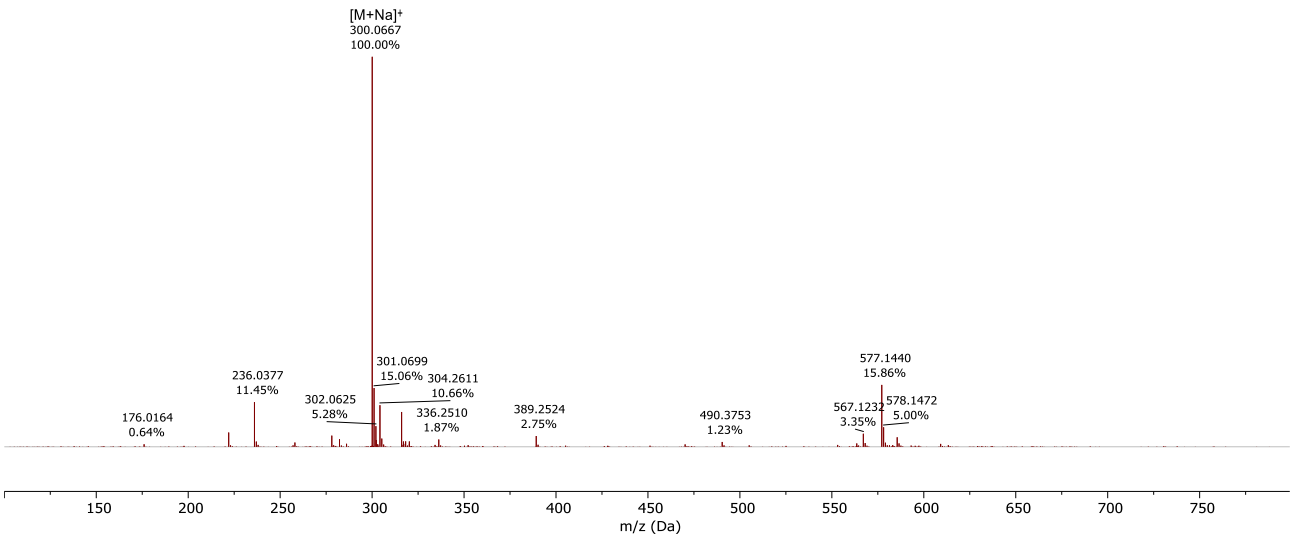

^{1}H-NMR (300 MHz, $CDCl_3$) of **5**

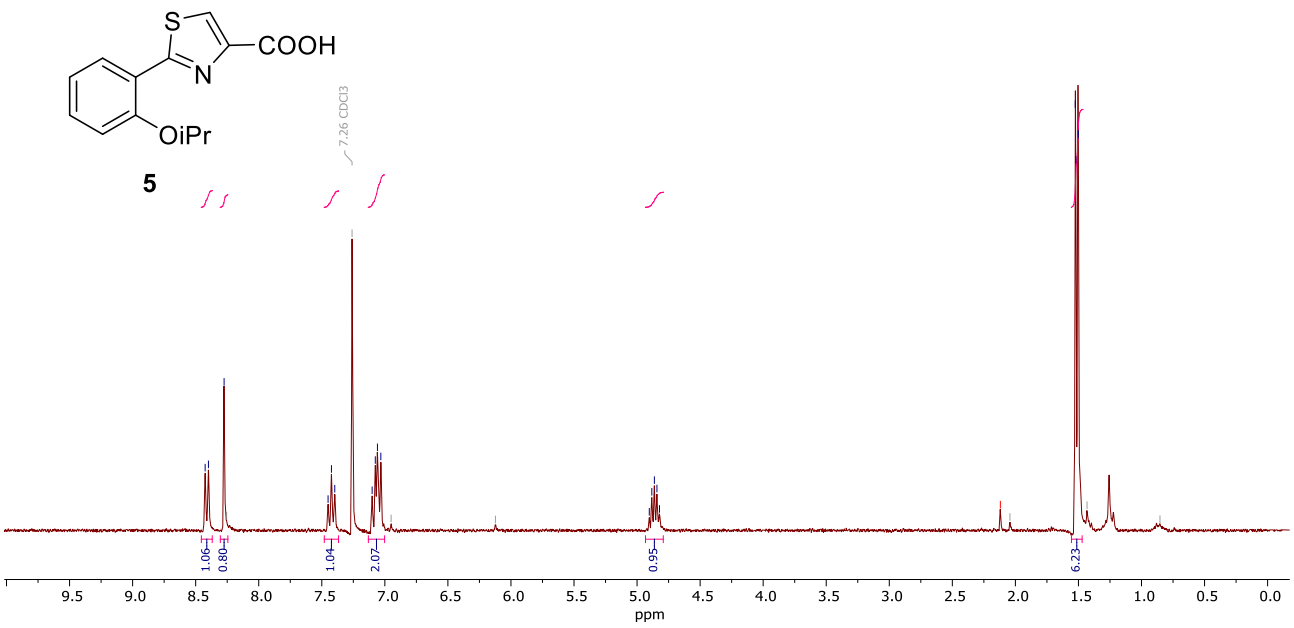

^{13}C-NMR (75 MHz, $CDCl_3$) of **5**

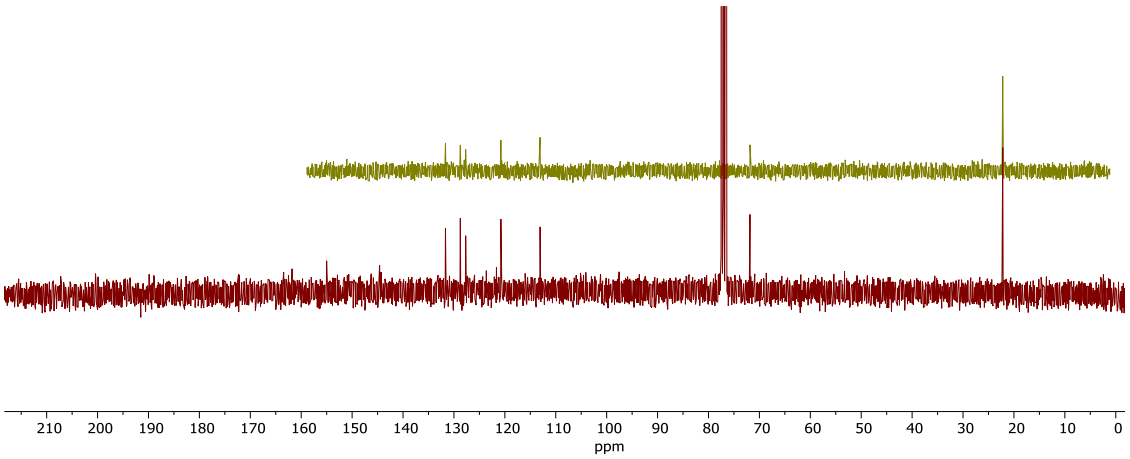

(+)- HRMS (ESI) of **5**

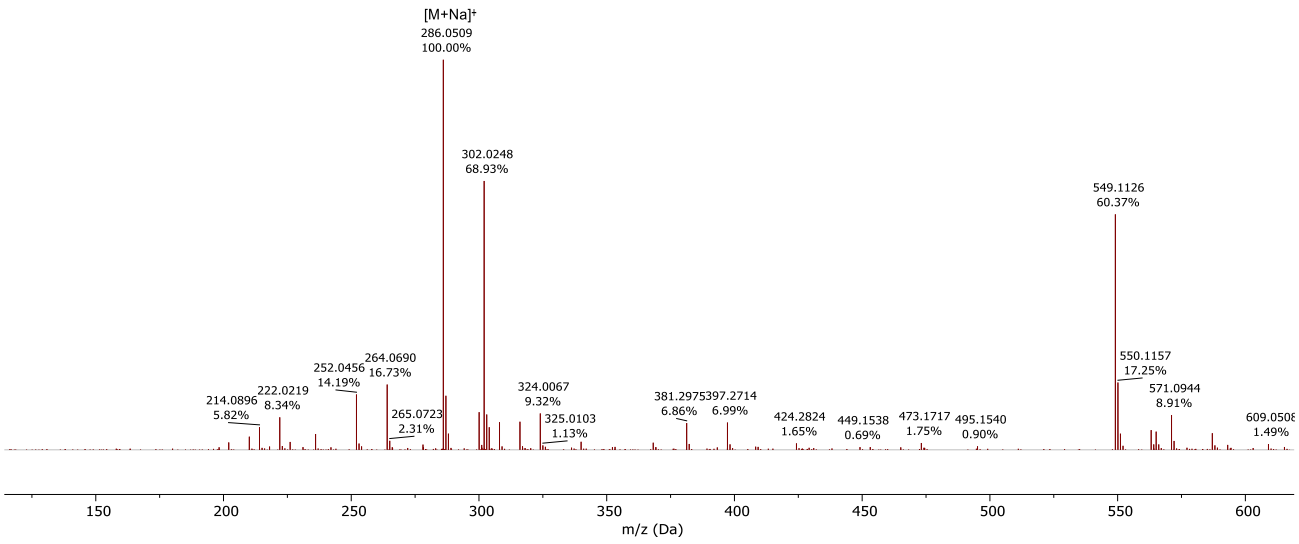

^{1}H-NMR (300 MHz, $CDCl_3$) of **6**

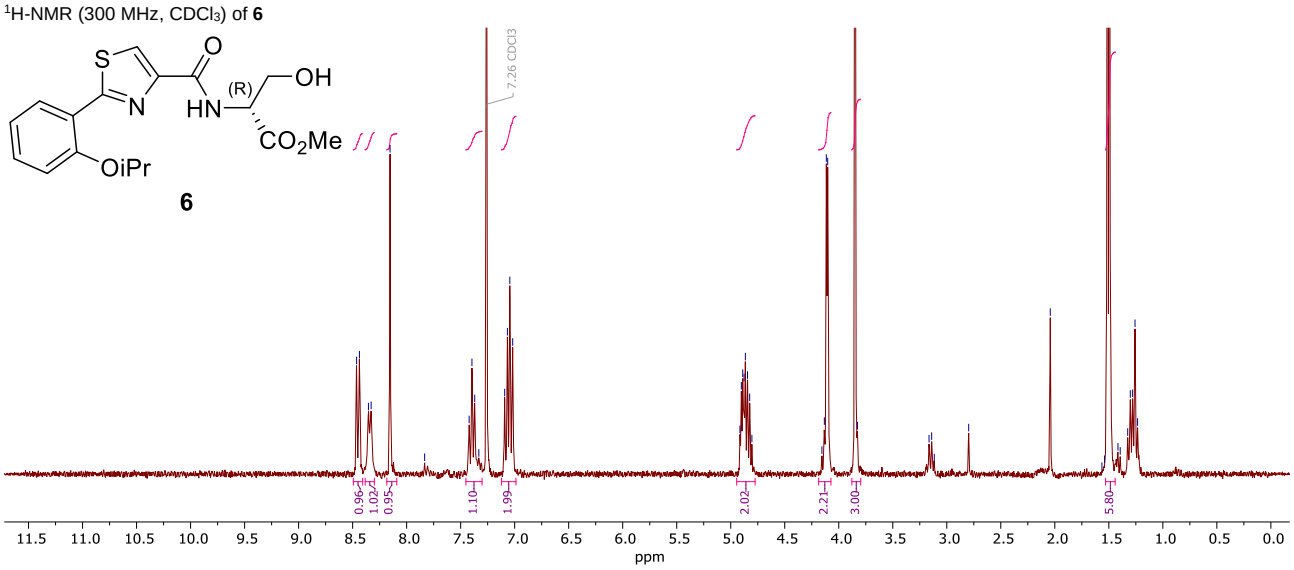

6

^{13}C-NMR (75 MHz, $CDCl_3$) of **6**

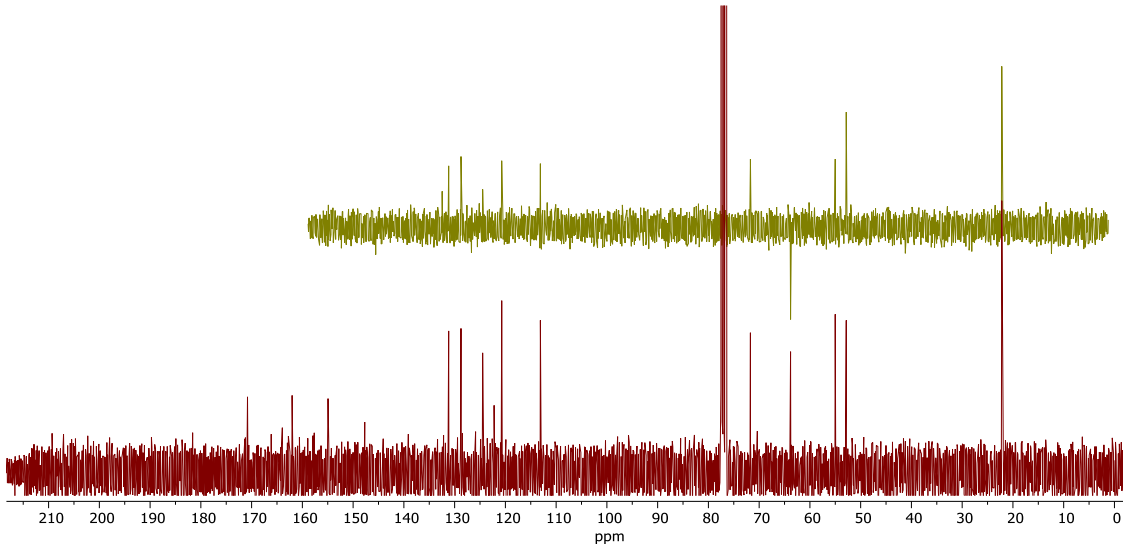

(+)-HRMS (ESI) of **6**

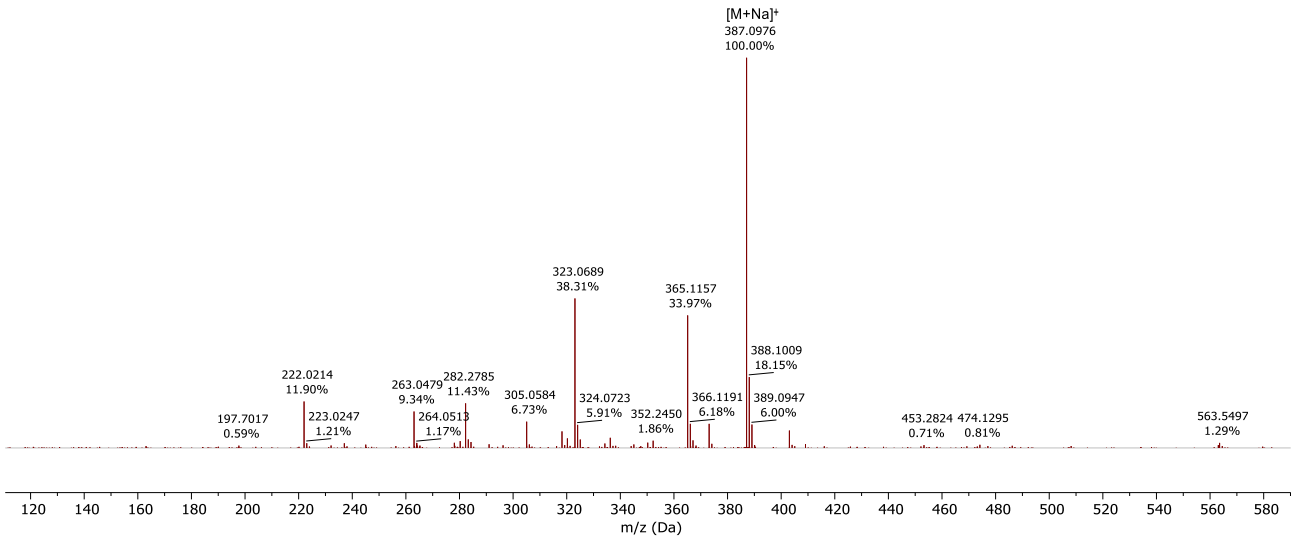

HSQC (500.13 MHz, CD_2Cl_2) of **6**